

## Volume Integral Equation Method Optimized for Black Carbon-Containing Aerosol Particles

NOBUHIRO, Moteki<sup>1\*</sup>

<sup>1</sup>Department of Earth and Planetary Science, The University of Tokyo

We propose a robust scheme of volume integral equation method (VIEM) for light scattering and absorption by black carbon-containing aerosol particles: the fractal-like aggregates of absorbing black carbon (BC) spherules that may be mixed with non-absorbing (or weakly absorbing) compounds. Conventionally, a particle volume has been uniformly approximated as a collection of small volume elements (dipoles) on a cubic lattice (CL). In the proposed scheme, each BC spherule is considered as a spherical dipole with original size, while remaining particle volume occupied by non-absorbing compounds is approximated by a collection of dipoles on a CL. We call this as Spherule-Retained-Cubic-Lattice (SRCL) scheme. For several model BC-containing particles, positive absorption bias of ~30% persistent in the CL scheme is successfully eliminated in SRCL scheme. The interaction matrix (i.e., discretized volume integral operator) associated with the SRCL scheme has less simple structure compared with that for CL scheme. We propose some key strategies for mitigating memory and computational costs in solving the matrix equation in the SRCL scheme.

Keywords: Atmospheric Radiation, Light Scattering Theory, Aerosol, Black Carbon

## Improved Technique to Measure the Size Distribution of Black Carbon Particles Suspended in Rainwater and Snow Samples

MORI, Tatsuhiko<sup>1\*</sup> ; OHATA, Sho<sup>1</sup> ; MOTTEKI, Nobuhiro<sup>1</sup> ; KONDO, Yutaka<sup>1</sup>

<sup>1</sup>Department of Earth and Planetary Science, Graduate School of Science, The University of Tokyo

Black carbon (BC) aerosols strongly absorb visible solar radiation. Quantitative understanding of wet removal process, which strongly affects the spatial distribution of BC, is important to improve our understandings on climate change. For this purpose, a measurement technique for BC in rainwater and in snow samples has been developed, as a combination of a nebulizer and a single particle soot photometer (SP2) (Ohata et al. 2011, 2013; Mori et al. 2014). We show two important improvements in this technique: (1) We have introduced a pneumatic nebulizer and experimentally confirmed its high extraction efficiency (~50%) independent of particle-size up to 2  $\mu\text{m}$ . (2) We have extended the upper limit of detectable BC size range by the SP2 from 0.9  $\mu\text{m}$  to 4  $\mu\text{m}$  by modifying a photo-detector for incandescence. Using this technique, we have measured the size-resolved mass concentration in air and in rainwater, simultaneously, during last summer in Tokyo. We observed significant amounts of BC particles with diameters larger than 1  $\mu\text{m}$  in rain samples. The correlation between BC mass concentration in air and in rainwater was high ( $r^2 = 0.59$ ), suggesting that the major sources of BC in rainwater were BC in the atmospheric planetary boundary layer. The size distribution of BC in rainwater was shifted to larger size as compared with that in air, indicating that larger BC particles in the air were removed more efficiently by precipitation.

Keywords: Black Carbon, Measurement, Wet deposition

## Measurements of the hygroscopicity and wet removal of black-carbon-containing particles in Tokyo

OHATA, Sho<sup>1\*</sup> ; NOBUHIRO, Moteki<sup>1</sup> ; MORI, Tatsuhiro<sup>1</sup> ; KOIKE, Makoto<sup>1</sup> ; TAKAMI, Akinori<sup>2</sup> ;  
KONDO, Yutaka<sup>1</sup>

<sup>1</sup>Department of Earth and Planetary Science, Graduate School of Science, The University of Tokyo, <sup>2</sup>Center for Regional Environmental Research, National Institute for Environmental Studies

Megacities are very large, concentrated anthropogenic sources of black carbon (BC) aerosols. Freshly emitted BC particles inside megacities affect local air quality and regional and global climate. The microphysical properties (e.g., number size distribution, coating thickness, and hygroscopicity) of atmospheric BC-containing particles are important because their efficiency of wet removal from the atmosphere can be highly dependent on these properties. In this study, we conducted intensive observations of the hygroscopicity and wet removal of BC-containing particles in the urban atmosphere of Tokyo during summer 2014. The number size distribution and coating thickness of BC-containing particles were measured with a standard Single Particle Soot Photometer (SP2). The hygroscopicity of BC-free and BC-containing particles was measured with a modified (humidified) SP2. In addition, the number size distribution of BC cores in rainwater was also measured with a nebulizer?SP2 system during rain events.

Throughout the observation period, for BC-containing particles with a dry diameter of about 200 nm, the particles with smaller BC fractions tended to represent greater water uptake, and the number fraction of the less hygroscopic (Growth factor <1.2 at 85% relative humidity) BC-containing particles was more than 70% of the total BC-containing particles. The measured average number size distribution of BC cores in rainwater was larger than that in the surface air before precipitation began, and the dependence of the wet removal of BC-containing particles on their BC-core sizes was successfully explained by the measured microphysical properties of BC-containing particles in the air and an assumed maximum supersaturation that the particles would have experienced during rain events. These measurement data indicated that BC-containing particles in Tokyo, especially particles with small BC cores (or with high critical supersaturation), were efficiently transported upward without being removed by precipitation.

Keywords: black carbon, hygroscopicity, wet removal

## Evaluation of Refueling emissions and its OFP

HIROYUKI, Yamada<sup>1\*</sup> ; INOMATA, Satoshi<sup>2</sup> ; TANIMOTO, Hiroshi<sup>2</sup>

<sup>1</sup>National Traffic Safety and Environment Laboratory, <sup>2</sup>National Institute for Environmental Study

Refueling emissions have been considered one of the main VOC sources in Japan. However there is only a few study which discuss the emission mechanism and its detailed effect on total VOC emissions in Japan. We performed the experiments using sealed housing evaporative determination (SHED) to evaluate the refueling emissions. For the measurement devices, we adopted not only total hydrocarbon, but also the composition analysis using proton transfer reaction plus switchable reagent ion mass spectrometry (PTR+SRI-MS) to estimate the ozone formation potential of refueling emissions. We also tested some prevention devices of refueling emissions.

Keywords: Refueling emissions, VOC, Ozone formation potential, PTR-MS

## Evaluation of black carbon radiative effect using a mixing state resolved three-dimensional model

MATSUI, Hitoshi<sup>1\*</sup>

<sup>1</sup>JAMSTEC

This study evaluates the uncertainties in black carbon (BC) and its optical and radiative parameters over East Asia (spring 2009) using a BC mixing state resolved three-dimensional model that can explicitly calculate BC processes in the atmosphere such as emissions, aging processes by condensation and coagulation, the enhancement of absorption and CCN activity by the aging, activation to cloud, and dry and wet deposition. The focus of this study is the uncertainties in the size distribution and the mixing state in emissions. One base case simulation and 14 sensitivity simulations are conducted to understand the variability of BC mass concentrations in column, absorption aerosol optical depth, and the radiative forcing by BC absorption due to the uncertainties in emissions. The variability of BC optical and radiative parameters is estimated to be 39-59%. This variability corresponds to BC absorption forcing from  $-12.6$  to  $6.5 \text{ W m}^{-2}$  at the surface and from  $4.3$  to  $6.6 \text{ W m}^{-2}$  at the top of atmosphere over East Asia, showing the importance of the treatment of the size and the mixing state in emissions. In contrast, the variability of BC mass concentrations is 17% and smaller than that of BC optical and radiative parameters. Therefore, BC optical and radiative parameters (BC mass concentrations) are more (less) sensitive to the size and the mixing state in emissions. This result shows that the following two points are important in the estimation of BC radiative forcing. The first is to reduce the uncertainties in the size and the mixing state in emissions. The second is to improve the representation of BC mixing state and the enhancement of BC absorption in aerosol models because most models do not treat them sufficiently. My analysis also shows that coagulation and lens effect (absorption enhancement due to the change in BC mixing state) play important roles to make the different variability between BC mass concentrations and BC optical and radiative parameters.

Keywords: aerosol, black carbon, mixing state, mixing state resolved three-dimensional model, absorption enhancement, radiative forcing

## Atmospheric Processing of Combustion Aerosols as a Source of Soluble Iron to the Open Ocean

ITO, Akinori<sup>1\*</sup>

<sup>1</sup>Japan Agency for Marine-Earth Science and Technology

Atmospheric processing of combustion aerosols may promote transformation of insoluble iron into soluble forms. Here, an explicit scheme for iron dissolution of combustion aerosols due to photochemical reactions with inorganic and organic acids in solution is implemented in an atmospheric chemistry transport model to estimate the atmospheric sources of bioavailable iron. The model results suggest that deposition of soluble iron from combustion sources contributes more than 40% of the total soluble iron deposition over significant portions of the open ocean in the Southern Hemisphere. A sensitivity simulation using half the iron dissolution rate for combustion aerosols results in relatively small decreases in soluble iron deposition in the ocean, compared with the large uncertainties associated with iron solubility at emission. More accurate quantification of the soluble iron burdens near the source regions and the open ocean is needed to improve the process-based understanding of the chemical modification of iron-containing minerals.

Keywords: Global environmental change, Atmospheric deposition, Soluble iron, Biomass burning

## Adjoint of the coupled Eulerian-Lagrangian transport model

BELIKOV, Dmitry<sup>1\*</sup> ; MAKSYUTOV, Shamil<sup>2</sup> ; YAREMCHUK, Alexey<sup>4</sup> ; GANSHIN, Alexander<sup>5</sup> ;  
ZHURAVLEV, Ruslan<sup>5</sup> ; AOKI, Shuji<sup>6</sup>

<sup>1</sup>National Institute of Polar Research, Tokyo, <sup>2</sup>National Institute for Environmental Studies, Tsukuba, <sup>3</sup>Tomsk State University, Tomsk, Russia, <sup>4</sup>N.N. Andreev Acoustic Institute, Moscow, Russia, <sup>5</sup>Central Aerological Observatory, Dolgoprudny, Russia, <sup>6</sup>Center for Atmospheric and Oceanic Studies, Graduate School of Science, Tohoku University, Sendai

We present the development of an inverse modeling system employing an adjoint of the global coupled transport model consisting of the National Institute for Environmental Studies (NIES) Eulerian transport model (TM) and the Lagrangian plume diffusion model (LPDM) FLEXPART. NIES TM is a three-dimensional atmospheric transport model, which solves the continuity equation for a number of atmospheric tracers on a grid spanning the entire globe. The Lagrangian component of the forward and adjoint models uses precalculated responses of the observed concentration to the surface fluxes and 3-D concentrations field simulated with the FLEXPART model. Construction of the adjoint of the Lagrangian part is less complicated, as LPDMs calculate the sensitivity of measurements to the surrounding emissions field by tracking a large number of particles backwards in time. Developing of the adjoint to Eulerian part required significant manual code modification owing to the structure and complexity of the NIES model.

The overall advantages of our method are follows:

1. No code modification of Lagrangian model is required, making it applicable to combination of global NIES TM and any Lagrangian model;
2. Once run, the Lagrangian output can be applied to any chemically neutral gas;
3. High-resolution results can be obtained over limited regions close to the monitoring sites (using the LPDM part), and at coarse resolution for the rest of the globe (using the Eulerian part), minimizing aggregation errors and computation cost.

The results are verified using a series of test experiments. These tests demonstrate the high accuracy of the NIES-FLEXPART adjoint when compared with direct forward sensitivity calculations. Adjoint of coupled NIES-FLEXPART model therefore combines the flux conservation and stability of an Eulerian finite difference of adjoint formulation with the flexibility, accuracy and high-resolution of a Lagrangian backward trajectory formulation.

The accuracy of the adjoint model is extensively verified by comparing adjoint to finite difference sensitivities. We show acceptable tolerance of agreement obtained. The potential for inverse modeling using the adjoint of NIES- FLEXPART coupled model is assessed in a data assimilation framework using simulated observations, demonstrating the feasibility of exploiting CO<sub>2</sub> measurements for optimizing CO<sub>2</sub> emission inventories.

Keywords: carbon cycle, atmospheric transport, adjoint model, inverse modeling

## Estimating source-receptor relationships of tropospheric ozone: On the importance of model horizontal resolution

SEKIYA, Takashi<sup>1\*</sup> ; SUDO, Kengo<sup>1</sup>

<sup>1</sup>Graduated School of Environmental Studies, Nagoya University

Ozone (O<sub>3</sub>) near the surface is harmful to human health and to vegetation including crops. It is recognized that intercontinental transport of air pollutants affects air quality over a region. Task Force on Hemispheric Transport of Air Pollutants (TF HTAP) coordinated a multi-model inter-comparison of 21 chemical transport models (CTMs) for assessing source-receptor relationships (i.e., the change in pollutants over a receptor region produced by change in emissions in a source region). Typical horizontal resolution of HTAP models was about 300 km. A coarse-resolution model tends to overpredict ozone chemical production (e.g., Wild and Prather, 2006). However, it is unclear how model horizontal resolution affects source-receptor relationships of tropospheric ozone. We estimated source-receptor relationships of tropospheric ozone using the CHASER global CTM (Sudo et al., 2002) with medium-resolution (T42; 2.8 deg. x 2.8 deg.) and high-resolution (T106; 1.1 deg. x 1.1 deg.). The CHASER model is also developed as an atmospheric chemistry component of the MIROC-ESM-CHEM earth system model, and simulates detailed chemistry in the troposphere and the stratosphere with aerosols simultaneously. We conducted a 2010 control simulation and a sensitivity simulation with 20% reduced emissions in East Asia to estimate source-receptor relationships. The model results show that 20% East Asian emission reductions decrease surface O<sub>3</sub> by 0.94 ppbv and by 0.75 ppbv over East Asia in spring respectively in the medium-resolution and high-resolution models. The East Asian emission perturbations also reduced surface O<sub>3</sub> by 0.27 ppbv and by 0.24 ppbv in spring over North America respectively in the medium-resolution and the high-resolution models. Our results suggest that the high-resolution model tends to predict smaller decreases in surface O<sub>3</sub> over East Asia and North America in response to the East Asian emission reductions.

### Reference

- Wild and Prather (2006), *J. Geophys. Res.*, 111, D11305, doi:10.1029/2005JD006605.  
Sudo et al. (2002), *J. Geophys. Res.*, 107, 10.1029/2001JD001113.

Keywords: tropospheric ozone, chemical transport model, source-receptor relationship, intercontinental transport



## Impacts of black carbon aging on its spatial distribution and radiative effect in the global scale

OSHIMA, Naga<sup>1\*</sup>; TANAKA, Taichu<sup>2</sup>; KOSHIRO, Tsuyoshi<sup>1</sup>; KAWAI, Hideaki<sup>1</sup>; DEUSHI, Makoto<sup>1</sup>; KOIKE, Makoto<sup>3</sup>; NOBUHIRO, Moteki<sup>3</sup>; KONDO, Yutaka<sup>3</sup>

<sup>1</sup>Meteorological Research Institute, <sup>2</sup>Global Environment and Marine Department, Japan Meteorological Agency, <sup>3</sup>Department of Earth and Planetary Science, Graduate School of Science, The University of Tokyo

Most aerosol components scatter solar radiation; however, black carbon (BC) aerosols efficiently absorb it and lead to heating of the atmosphere. Because of these effects, the role of BC particles in the climate system has been recognized to be particularly important. Freshly emitted hydrophobic BC particles become internally mixed with other water-soluble compounds through aging processes and they are converted to hydrophilic BC. Internal mixing with sufficient water-soluble compounds enhances the BC absorption efficiency of solar radiation, and the hydrophilic BC particles are able to serve as cloud condensation nuclei (CCN), which can be removed from the atmosphere by precipitation. Consequently, aging processes of BC influence its atmospheric lifetime and play an important role for the spatial distributions of BC and its radiative effects. However, a simple approach using constant values of the conversion rate from hydrophobic BC to hydrophilic BC (such as 24 hours) has been widely used in most global models and there were large uncertainties in estimating the spatial distribution of BC and its radiative forcing in previous studies. Recent studies pointed out the necessity of an advanced parameterization of BC aging processes to improve the quantitative estimation of the climate impacts of BC.

Recently, Oshima and Koike [2013] developed a new parameterization of BC aging based on the physical and chemical processes. In this parameterization, the conversion rate from hydrophobic BC to hydrophilic BC is expressed as a production rate of condensed materials normalized by the hydrophobic BC mass concentration. In this study, we applied this parameterization to the global-scale aerosol model MASINGAR-mk2 included in the MRI's earth system model [Yukimoto et al., 2012], which enables the representation of spatial and temporal variations of the conversion rate of BC aging depending on atmospheric conditions (the original approach assumed the constant conversion rate of 1.2 days).

We performed the model calculation with the BC aging parameterization for 2008-2009. We find that the conversion time scales from hydrophobic BC to hydrophilic BC exhibit distinct spatial variations and they were approximately one day and one week over the source regions in East Asia and the remote regions in the Arctic, respectively. We also performed the model calculation with the constant conversion rate (1.2 days) for the comparison. Over the source regions in East Asia, both calculations give small differences in BC mass concentrations and they reproduced the seasonal variations of BC mass concentrations observed by the surface measurements reasonably well. On the other hand, the both calculations give large differences in BC mass concentrations over the Arctic regions and the calculation with the parameterization improved the prediction of the BC mass concentration, which was underestimated in the constant-rate calculation.

The direct radiative forcing by BC (annually and globally averaged at the top of atmosphere) was approximately  $0.3 \text{ W m}^{-2}$  for the calculation with the parameterization (approximately  $0.2 \text{ W m}^{-2}$  for the constant-rate calculation). This result indicates that the aging process of BC in the micro-scale can significantly impact on the spatial distribution and radiative forcing in the global-scale through the parameterization. However, the calculations shown in this study do not take into account the enhancement of BC light absorption due to coatings and they may underestimate the direct radiative forcing. We will introduce model results including the enhancement effect in this presentation.

### References

- Oshima, N., and M. Koike (2013), *Geosci. Model Dev.*, **6**, 263-282, doi:10.5194/gmd-6-263-2013.  
Yukimoto, S., et al. (2012), *J. Meteor. Soc. Japan*, **90A**, 23-64, doi:10.2151/jmsj.2012-A02.

Keywords: Aerosol, Black carbon, Global aerosol model, Aging process, Transport, Radiative effects

## Interannual variabilities in tropospheric constituents during 2000-2013 simulated in a chemistry-aerosol coupled climate

SUDO, Kengo<sup>1\*</sup> ; ITO, Akihiko<sup>3</sup>

<sup>1</sup>Graduate School of Environmental Studies, Nagoya University, <sup>2</sup>Japan Marine-Earth Science and Technology, <sup>3</sup>National Institute of Environmental Studies

Global distributions and abundances of tropospheric constituents ( $O_3$ ,  $CH_4$ ,  $NO_y$ ,  $CO$ , VOCs,  $NH_x$ ,  $SO_x$  and aerosols) interannually change under the influences of meteorology (transport, temperature, water vapor, clouds, rain, etc.) and emissions from anthropogenic/natural sources and biomass burning. In this study, we investigate interannual variability of tropospheric constituents during the years 2000 to 2013 in a chemistry-aerosol coupled climate model. The base chemical model used in this study is CHASER (Sudo et al., 2002, 2007) coupled with the aerosol model SPRINTARS (Takemura et al., 2006). The CHASER model, also developed in the framework of the MIROC earth system model (MIROC-ESM-CHEM), simulates detailed chemistry in the troposphere and stratosphere with an on-line aerosol simulation including production of particulate nitrate and SOA. We use the NCEP reanalysis data (FNL) for constraining the model's meteorology. Anthropogenic and biomass burning emissions are specified using the HTAP2 and MAC inventories, respectively. For biogenic VOCs emissions, we employ calculation by the land ecosystem/trace gas emission model VISIT (Ito et al., 2008). Our results show that temporal variability (anomaly) in surface and lower tropospheric ozone very clearly correlates with that in CO especially in NH, indicating principal importance of biomass burning emission in determining near-surface  $O_3$  variability; surface PM ( $PM_{2.5}$ ) in NH also coincides with CO. Changes in middle to upper tropospheric  $O_3$ , on the other hand, basically respond to variability in transport from the stratosphere and lightning  $NO_x$  production. It is also demonstrated that temporal variability in tropospheric mean OH is largely controlled by tropospheric abundances of  $O_3$ , CO, and water vapor.

Keywords: tropospheric ozone, aerosol,  $PM_{2.5}$ , methane, oxidation capacity, chemistry climate model

## Numerical Analysis of total nitrate deposition over marginal seas of Japan

ITAHASHI, Syuichi<sup>1\*</sup> ; HAYAMI, Hiroshi<sup>1</sup> ; UNO, Itsushi<sup>2</sup> ; UEMATSU, Mitsuo<sup>3</sup>

<sup>1</sup>Environmental Science Research Laboratory, Central Research Institute of Electric Power Industry, <sup>2</sup>Research Institute of Applied Mechanics, Kyushu University, <sup>3</sup>Atmosphere and Ocean Research Institute, The University of Tokyo

In China, due to the expanded economy growth, anthropogenic NO<sub>x</sub> emissions increased more than twofold between 2000 and 2010. Aerosol nitrate and gas-phase nitrate produced from NO<sub>x</sub> deposit above ocean during long-range transport process, and the impacts on ocean-ecosystem are apprehensive. In this study, on the basis of regional chemical transport which can treat the detailed behavior of air pollutants, we investigated the deposition of total nitrate from atmosphere into marginal seas of Japan. Analyzed period was on the year from 2002 to 2004. Chemical transport model can well reproduce the atmospheric concentration and wet deposition amount by comparing the ground-based observation dataset of EANET. Above East China Sea (ECS), three-year averaged deposition amount of total nitrate was 252 Gg-N/year. Dry and wet deposition process respectively accounted 60% and 40%. Deposition amount of fine-mode nitrate and coarse-mode nitrate respectively attributed 22% and 50%, and the rest of 28% was gas-phase nitrate. During these period, anthropogenic NO<sub>x</sub> emissions from China was 5377 Gg-N/year, therefore, the deposition amount of total nitrate over ECS was corresponded to 4.7%. Taking into account that the deposition amount above China was 2039 Gg-N/year, the deposition amount over ECS was identified as 7.5% against to anthropogenic NO<sub>x</sub> emissions from China. In the conference presentation, we would like to present the analyzed results over Sea of Japan, Yellow Sea, and Pacific open oceans, and discuss the correspondence with anthropogenic NO<sub>x</sub> emissions from China.

Keywords: marginal seas of Japan, aerosol nitrate, gas-phase nitrate, deposition amount, chemical transport model

## Contribution of Siberian forest fires to PM<sub>2.5</sub> pollution in Japan

IKEDA, Kohei<sup>1\*</sup> ; TANIMOTO, Hiroshi<sup>1</sup>

<sup>1</sup>National Institute for Environmental Studies

We examined the contribution from Siberian forest fires to PM<sub>2.5</sub> pollution in Japan using a regional chemical transport model. In May 2003, several events resulting in PM<sub>2.5</sub> concentrations exceeding Japan's air quality standard for daily mean value ( $35 \mu\text{g}/\text{m}^3$ ) were observed at Rishiri in northern Japan. The model generally well reproduced the temporal variations of PM<sub>2.5</sub> including the elevated events. The simulations demonstrated that the PM<sub>2.5</sub> enhancements during the events were mostly attributed to biomass burning in Siberia, suggesting that the contribution from Siberian forest fires had a critical impact on the high PM<sub>2.5</sub> days ( $>35 \mu\text{g}/\text{m}^3$ ). The contributions from Siberian biomass burning to the monthly mean PM<sub>2.5</sub> concentrations were estimated to be 64% at Rishiri and 45% at both Nonodake and Oki located in eastern and western Japan, respectively, suggesting that Siberian forest fires had a large impact on air quality for the whole of Japan. Especially at Rishiri, the observed PM<sub>2.5</sub> concentrations and aerosol optical depth (AOD) from MODIS in May 2003 were much larger than those of the 10-year average in May from 2001 to 2010. The trend in horizontal distribution for May 2003 was opposite to the long-term average; PM<sub>2.5</sub> and AOD in May 2003 were the highest in northern Japan.

Keywords: PM<sub>2.5</sub>, aerosol, forest fires, Siberia, transboundary pollution

## Observations of O<sub>3</sub>, CO, CO<sub>2</sub> and CH<sub>4</sub> concentrations at Happo and estimations of the source by chemical transport model

OKAMOTO, Sachiko<sup>1\*</sup> ; TANIMOTO, Hiroshi<sup>1</sup> ; NARA, Hideki<sup>1</sup> ; IKEDA, Kohei<sup>1</sup> ; YAMAJI, Kazuyo<sup>2</sup>

<sup>1</sup>National Institute for Environmental Studies, <sup>2</sup>Kobe University

A large increase in tropospheric O<sub>3</sub> concentrations was observed during spring for the period from 1998 to 2006 at Mt. Happo Observatory (36.7°N, 137.8°E, 1840 m asl), which is one of the Acid Deposition Monitoring Network in East Asia (EANET) stations (Tanimoto, 2009). The increase in the springtime O<sub>3</sub> reproduced by a regional chemistry-transport model incorporating the updated anthropogenic emissions inventory in East Asia can only explain about half of the observed O<sub>3</sub> increase (Tanimoto et al., 2009). On the other hand, previous source-receptor analysis by a global chemistry-transport model indicated that the contributions of local and regional sources can vary, depending on individual episodes (Wild et al., 2004). For better understanding of the discrepancies between the model prediction and observational evidence, it is necessary to better characterize air masses at Mt. Happo by simultaneous measurements of additional tracers like CO, CO<sub>2</sub>, and CH<sub>4</sub>.

Starting in July 2013, we have made continuous measurements of CO, CO<sub>2</sub> and CH<sub>4</sub> as well as O<sub>3</sub> at Mt. Happo. We found that the O<sub>3</sub> levels at Mt. Happo increased until 2007, and then the increase slowed down and now decreased to the same level as in 1990s. The CO concentrations observed for the period of 2013-2014 was found to be lower than those in 1990s. In particular, the current CO levels were 50 ppbv lower than in 1990s during summer. In total, 44 events associated with O<sub>3</sub> enhancement were identified for the period from July 2013 to August 2014. Correlations of CO with CO<sub>2</sub> and CH<sub>4</sub> with CO<sub>2</sub> were used to identify possible source regions for individual episodes. Emission ratios ( $\Delta\text{CO}/\Delta\text{CO}_2$  and  $\Delta\text{CH}_4/\Delta\text{CO}_2$ ) were calculated in each event, and compared with the ratios estimated by the regional emission inventory in Asia (REAS; Kurokawa et al., 2013). There is a discrepancy between two emission ratios. The  $\Delta\text{CO}/\Delta\text{CO}_2$  indicated that most events except summer were affected by the emissions from East Asia. On the other hand, the  $\Delta\text{CH}_4/\Delta\text{CO}_2$  indicated that most of events were caused by the emissions from Japan and Korea. It is difficult to identify the source regions by the ratios only.

We compared the observations with the model calculations by CMAQ v4.7.1, a regional chemistry-transport model, with the horizontal and vertical resolutions of 80 km and 37 layers, respectively. The model calculations well reproduced variability and seasonal changes of CO. For O<sub>3</sub>, although the model prediction was higher than the observed, in particular during the summer season, the model reproduced the O<sub>3</sub> enhancement events reasonably well. The source regions inferred by the model will be discussed in the presentation.

Keywords: ozone, carbon monoxide, methane, carbon dioxide

## Long-term variations of atmospheric methane concentration over Siberia derived from aircraft and tower measurements

SASAKAWA, Motoki<sup>1\*</sup>; MACHIDA, Toshinobu<sup>1</sup>; ITO, Akihiko<sup>1</sup>; TSUDA, Noritsugu<sup>2</sup>; ARSHINOV, Mikhail<sup>3</sup>; DAVYDOV, Denis<sup>3</sup>; FOFONOV, Alexandrov<sup>3</sup>; KRASNOV, Oleg<sup>3</sup>; PATRA, Prabir<sup>4</sup>; ISHIJIMA, Kentaro<sup>4</sup>

<sup>1</sup>National Institute for Environmental Studies, <sup>2</sup>Global Environmental Forum, <sup>3</sup>V.E. Zuev Institute of Atmospheric Optics, Russian Academy of Sciences, <sup>4</sup>Japan Agency for Marine-Earth Science and Technology

Methane measurements over Siberia are crucial for estimating global CH<sub>4</sub> emissions since Siberia is estimated to contain over 100 million ha of wetlands. We have been acquiring long-term records of atmospheric CH<sub>4</sub> concentration in Siberia at 3 sites (Surgut, Novosibirsk, Yakutsk) using aircraft since 1993 and at a tower network since 2004 (JR-STATION: Japan-Russia Siberian Tall Tower Inland Observation Network, Sasakawa *et al.*, 2010, 2012). Observed CH<sub>4</sub> concentrations at the tower sites in West Siberia showed much higher than those observed at coastal background sites operated by NOAA in northern high latitudinal zone. They also exhibited clear seasonal cycle with double maxima in winter and summer. However increasing trend observed in background sites did not appear in tower data due to high variability in concentration during summer and winter. On the other hand, aircraft data did not have clear seasonal cycle but showed obvious increasing trend. Global stagnation in rise of CH<sub>4</sub> concentration around 2000-2006 was observed in aircraft data over taiga sites (Novosibirsk, Yakutsk) but not clear over wetland site (Surgut). In Surgut, vertical difference of CH<sub>4</sub> concentration in recent years between 1 km and 5.5 km altitude data decreased less than 2/3 of that in early 1990's. This weakening vertical gradient appeared in other altitude data (0.5-4 km) as well. Simulation results with a chemistry-transport model (ACTM; Patra *et al.*, 2009) suggested that transport influence on this trend could be small. A regional emission tagged tracer simulation with the ACTM (Umezawa *et al.*, 2014) indicated that the CH<sub>4</sub> emissions from West Siberia and Europe could produce most extent of the vertical gradient. This finding thus suggested that the sum of dominant emissions decreased in these 20 years.

### References

- Patra *et al.*, *J. Meteorol. Soc. Jpn.*, **87**(4), 635-663, 2009.  
Sasakawa *et al.*, *Tellus*, **62B**, 403-416, 2010.  
Sasakawa *et al.*, *Tellus*, **64B**, 17514, doi:10.3402/tellusb.v64i0.17514, 2012.  
Umezawa *et al.*, *Tellus*, **66B**, 23837, 2014.

Keywords: Siberia, methane, tower network, aircraft observation

## Variations of atmospheric methane concentration and its carbon and hydrogen isotopic ratios at Churchill, Canada

FUJITA, Ryo<sup>1\*</sup> ; MORIMOTO, Shinji<sup>1</sup> ; UMEZAWA, Taku<sup>2</sup> ; DOUG, Worthy<sup>3</sup> ; AOKI, Shuji<sup>1</sup> ; NAKAZAWA, Takakiyo<sup>1</sup>

<sup>1</sup>Center for Atmospheric and Oceanic Studies, Graduate School of Science, Tohoku University, <sup>2</sup>National Institute for Environmental Studies, <sup>3</sup>Environment Canada

Methane (CH<sub>4</sub>) is the second most important anthropogenic greenhouse gas after CO<sub>2</sub>. High-precision measurements of carbon and hydrogen stable isotopic ratios of CH<sub>4</sub> ( $\delta^{13}\text{CH}_4$  and  $\delta\text{D-CH}_4$ ) provide additional constraints to contributions of individual CH<sub>4</sub> sources to atmospheric CH<sub>4</sub> variations. Since 2007, we have conducted an air-sampling program at Churchill, Canada (58.44°N, 93.50°W) on the northern perimeter of the Hudson Bay Lowland, the second largest wetland area in the world i.e. one of the most important CH<sub>4</sub> source regions at northern high latitudes. In this study, we present temporal variations of CH<sub>4</sub>,  $\delta^{13}\text{CH}_4$  and  $\delta\text{D-CH}_4$  at this site.

We observed long-term increase in the CH<sub>4</sub> concentrations at Churchill since 2007, which is consistent with the trend reported by the global observation networks such as NOAA/ESRL/GMD. The CH<sub>4</sub> concentration at Churchill is generally higher than that at Ny-Ålesund (78.55°N, 11.56°E), a northern high-latitude background station away from regional CH<sub>4</sub> sources. On the other hand,  $\delta^{13}\text{CH}_4$  and  $\delta\text{D-CH}_4$  at Churchill are lower than those at Ny-Ålesund, plausibly reflecting regional CH<sub>4</sub> emissions. Clear seasonal cycles of the CH<sub>4</sub> concentration and  $\delta^{13}\text{CH}_4$  were observed; seasonal maximum and minimum of the CH<sub>4</sub> concentration take place in January-February and June-July, respectively, while those of  $\delta^{13}\text{CH}_4$  were in May and October, respectively. Seasonal cycles of  $\delta\text{D-CH}_4$  were obscure but observable. The seasonal phases of these variables were up to one month earlier than those at Ny-Ålesund. The cause of the difference could be attributable to wetland emissions in the surrounding region. Short-term variations of the CH<sub>4</sub> concentration were observed year around, but pronounced in summer. By inspecting relationships between the CH<sub>4</sub> concentration and the isotopic ratios, we found that the predominant CH<sub>4</sub> source of the short-term CH<sub>4</sub> variations is wetlands in summer but fossil fuels in winter.

Keywords: methane, carbon and hydrogen isotopic ratios, Hudson Bay Lowland, wetlands

## Temporal variation of methane profile observed with FTIR at Tsukuba

MURATA, Isao<sup>1\*</sup> ; NAKAJIMA, Hideaki<sup>2</sup> ; MORINO, Isamu<sup>3</sup>

<sup>1</sup>Graduate School of Environmental Studies, Tohoku University, <sup>2</sup>Council for Science, Technology and Innovation, Cabinet Office, Government of Japan, <sup>3</sup>National Institute for Environmental Studies

The vertical profiles of CH<sub>4</sub> have been observed with high-resolution Fourier transform spectrometer at Tsukuba, Japan since 2001. SFIT2 spectral fitting program was used to derive the vertical profiles from 3 spectral regions in 3 micrometer region.

CH<sub>4</sub> is the second important contributor of the anthropogenically enhanced greenhouse effect but there are many uncertainties in the source variations.

Daily averaged CH<sub>4</sub> total column density kept a level from 2001 to 2006, then increased from 2007 to 2008, and again kept a level from 2009 to 2014. Tropopause height shows no significant change between before and after 2007, indicating stable dynamical situation. Derived CH<sub>4</sub> profiles show that the increase occurred mainly in the troposphere.

Keywords: FTIR, Greenhouse Gas, Methane



## Atmospheric methane measurement by open-path laser methane instrument at paddy fields in India

HIDEMORI, Takehiro<sup>1\*</sup>; MATSUMI, Yutaka<sup>1</sup>; NAKAYAMA, Tomoki<sup>1</sup>; SASAGO, Hiroshi<sup>1</sup>; KAWASAKI, Masahiro<sup>1</sup>; IMASU, Ryoichi<sup>2</sup>; ADACHI, Minaco<sup>3</sup>; TAKEUCHI, Wataru<sup>3</sup>; TERAOKA, Yukio<sup>4</sup>; NOMURA, Shohei<sup>4</sup>; MACHIDA, Toshinobu<sup>4</sup>; TAKAHASHI, Kenshi<sup>5</sup>; DHAKA, Surendra<sup>6</sup>; SINGH, Jagmohan<sup>6</sup>

<sup>1</sup>Solar-Terrestrial Environment Laboratory, Nagoya University, <sup>2</sup>Atmosphere and Ocean Research Institute, The University of Tokyo, <sup>3</sup>The University of Tokyo, Institute of Industrial Science, <sup>4</sup>National Institute for Environmental Studies, <sup>5</sup>Research Institute for Sustainable Humanosphere, Kyoto University, <sup>6</sup>Rajdhani College, Univ. of Delhi

Methane is the second important greenhouse gas after carbon dioxide, and increasing importance to the Earth's radiative budget. To better quantify methane emissions, their regional and temporal distribution, and attribution to the different methane sources is needed. Satellite observations offer the possibility of sensing methane globally and retrieving methane abundances in remote areas and can help with interpretation of sparse ground based measurement. In southeast and south Asia, the previous satellite observations suggest that the emission from rice paddies is significant and important source of methane during rainy season. However, there are large uncertainties in quantitative estimation of methane emission in these areas and there are needs for more certification between satellite and ground based measurements. In remote areas with insufficient infrastructure, air sampling and subsequently analysis are typical and reliable method for gas analysis. We developed the methane concentration measurement system which can make a continuous observation to interpolate the data of sampled air between each sampling period and we have operated the developed system at rural area in India.

The developed measurement system consists of gas sensor, power supply, data logger, remote control instruments and telecommunication equipment. The methane gas sensor is used a laser methane measurement instrument (LaserMethane, ANRITSU CORPORATION) which is a portable detector with low electric consumption, easy maintenance, and outdoor use. Remote sensing of methane is accomplished by means of infrared absorption spectroscopy with near-IR diode laser using reflected light from a reflector located at several tens meters away from the detector. High sensitivity is achieved by the second-harmonic detection of wavelength modulation spectroscopy. It can quickly and selectively detect the integral methane concentration on the optical path of the laser beam. To measure the methane concentration at paddy field in India, the methane measurement system was installed at rural area (Sonapat, Haryana) on the north of Delhi and has been operated since the winter of 2014. The air sampling along with our measurement has been carried out once a week currently. The methane concentration from the laser instrument can be corrected with the more precise value of the sampled air. To establish how to correct the data and calibrate the system, we performed both of laboratory experiment and field measurement. We will present about the development of the open-path laser methane measurement system and the recent results of field measurement in India.

Keywords: methane, open-path laser spectroscopy, paddy field, India

## Relationship between interannual variation in the changing rate of APO trend at Cape Ochi-ishi and PDO

TOHJIMA, Yasunori<sup>1\*</sup> ; MUKAI, Hitoshi<sup>1</sup> ; MACHIDA, Toshinobu<sup>1</sup> ; TERAOKA, Yukio<sup>1</sup>

<sup>1</sup>National Institute for Environmental Studies

Since atmospheric potential oxygen ( $APO = O_2 + 1.1 \times CO_2$ ) mainly reflects the air-sea gas exchange of  $O_2$  and  $CO_2$  by definition, the spatio-temporal variations in APO are expected to constrain the ocean biogeochemical process and dynamics. Here we examine the relationship between temporal variations in APO trend observed at Cape Ochi-ishi (COI; 43.2°N, 145.5°E) and the Pacific Decadal Oscillation (PDO) index to investigate the causes for the inter-annual variations in the APO trend. The PDO is a long-term Pacific climate variability, having two extreme phases which is classified by basin-scale patterns of the sea surface temperature (SST) anomaly. When the SST anomalies are cool in the northern North Pacific and warm in the tropical Pacific, the PDO index has positive value. And the opposite pattern of the SST anomalies correspond to the negative PDO index. The cool SST enhances the ocean vertical ventilation which brings deeper waters with depleted  $O_2$  to the surface, causing the  $O_2$  ingassing. The cool SST also enhances the ingassing flux by increasing gas solubility. To the contrary, the enhanced ocean vertical ventilation brings the subsurface nutrients to the surface, enhancing the  $O_2$  outgassing through the increase in the ocean primary production. Thus, the correlation analysis between the changing rate of the APO trend ( $dAPO/dt$ ) at COI and the PDO index would allow us to investigate how the SST anomaly in the northern North Pacific affect the air-sea gas exchanges. Unfortunately, there is no significant correlation between  $dAPO/dt$  and the PDO index. However, when  $dAPO/dt$  and the PDO index are decomposed into the middle ( $0.3 < f < 0.6$  cycle/yr) and low ( $f < 0.3$  cycle/yr) frequency domains by using a digital filtering technique, the scatter plots of the middle-term and long-term variations show significant negative and positive correlations, respectively. These results might suggest that the ventilation/thermal effect is dominant for the middle-term SST variation while the biotic effect exceeds it for the long-term SST variation.

Keywords: APO, atmospheric oxygen, PDO, atmospheric  $CO_2$ , air-sea gas exchange

## Variations in the atmospheric Ar/N<sub>2</sub> and APO observed at Tsukuba, Ochi-Ishi, Hateruma and Minamitorishima, Japan

ISHIDOYA, Shigeyuki<sup>1\*</sup>; MURAYAMA, Shohei<sup>1</sup>; TOHJIMA, Yasunori<sup>2</sup>; TSUBOI, Kazuhiro<sup>3</sup>; MATSUEDA, Hidekazu<sup>3</sup>; TAGUCHI, Shoichi<sup>1</sup>; PATRA, Prabir<sup>4</sup>; KONDO, Hiroaki<sup>1</sup>

<sup>1</sup>National Institute of Advanced Industrial Science and Technology (AIST), <sup>2</sup>National Institute for Environmental Studies (NIES), <sup>3</sup>Meteorological Research Institute (MRI), <sup>4</sup>Japan Agency for Marine-Earth Science and Technology (JAMSTEC)

Atmospheric Ar/N<sub>2</sub> ratio is a unique tracer of spatiotemporally-integrated air-sea heat fluxes, and expected to be a new tool to validate changes in the global ocean heat content (e.g. Keeling et al. 2004; Cassar et al., 2008). The Ar/N<sub>2</sub> ratio is also useful to estimate thermal and biological components of Atmospheric Potential Oxygen (APO = O<sub>2</sub> + 1.1xCO<sub>2</sub>) separately, so that it will contribute to better understanding of the oceanic carbon cycle. Therefore, we have developed a high-precision measurement system of the atmospheric Ar/N<sub>2</sub> ratio and APO (Ishidoya and Murayama, 2014), which is applicable both for continuous observations and analyses of discrete flask air samples, and started systematic observations of the Ar/N<sub>2</sub> and APO at Tsukuba (36N, 140E) and Hateruma Island (24N, 124E), Japan since 2012 and at Cape Ochi-Ishi (43N, 146E) and Minamitorishima Island (24N, 154E), Japan since 2013. Clear seasonal cycles of the Ar/N<sub>2</sub> ratio were observed at all the sites, and the peak-to-peak amplitudes of the seasonal cycles were in the range of 15 - 50 per meg. The observed amplitudes were found to be significantly larger than those calculated using atmospheric transport models and the seasonal air-sea N<sub>2</sub> fluxes climatology (TransCom fluxes; Garcia and Keeling et al., 2001) with a scaling factor to convert changes in the atmospheric N<sub>2</sub> concentration to those in the Ar/N<sub>2</sub> ratio (Blaine, 2005). We will also present preliminary estimations of the thermal and the biological APO at our sites by using the observed seasonal Ar/N<sub>2</sub> and APO cycles.

### Acknowledgements

We would like to acknowledge N. Oda and F. Shimano, Global Environmental Forum, and many staffs of Japan Meteorological Agency for their supporting the observations.

### References

- Blaine, T. (2005) Continuous Measurements of Atmospheric Argon/Nitrogen as a Tracer of Air-Sea Heat Flux: Models, Methods, and Data. PhD Thesis, University of California, San Diego.
- Cassar, N. et al. (2008) An improved comparison of atmospheric Ar/N<sub>2</sub> time series and paired ocean-atmosphere model predictions. *J. Geophys. Res.*, 113, D21122. DOI: 10.1029/2008JD009817.
- Garcia, H. & Keeling, R. (2001) On the global oxygen anomaly and air-sea flux. *J. Geophys. Res.*, 106, 31155-31166.
- Ishidoya, S. & Murayama, S. (2014) Development of high precision continuous measuring system of the atmospheric O<sub>2</sub>/N<sub>2</sub> and Ar/N<sub>2</sub> ratios and its application to the observation in Tsukuba, Japan. *Tellus B*, 66, 22574, <http://dx.doi.org/10.3402/tellusb.v66.22574>.
- Keeling, R. et al. (2004) Measurement of changes in atmospheric Ar/N<sub>2</sub> ratio using a rapid-switching, single-capillary mass spectrometer system. *Tellus B*, 56, 322-338.

Keywords: Atmospheric Ar/N<sub>2</sub> ratio, Atmospheric Potential Oxygen (APO), Air-sea heat flux

## Seasonal variations of nitrogen and oxygen isotopic signature of atmospheric nitrate in coastal Antarctica

ISHINO, Sakiko<sup>1\*</sup> ; HATTORI, Shohei<sup>1</sup> ; CAILLON, Nicolas<sup>2</sup> ; BARBERO, Albane<sup>2</sup> ; GAUTIER, Elsa<sup>2</sup> ;  
JOURDAIN, Bruno<sup>2</sup> ; PREUNKERT, Susanne<sup>2</sup> ; LEGRAND, Michel<sup>2</sup> ; YOSHIDA, Naohiro<sup>1</sup> ; SAVARINO, Joel<sup>2</sup>

<sup>1</sup>Interdisciplinary Graduate School of Science and Engineering, Tokyo Institute of Technology, Japan, <sup>2</sup>Universite Grenoble Alpes/CNRS, LGGE, F-38000 Grenoble, France

Nitrate ( $\text{NO}_3^-$ ) is the end-product of oxidation of nitrogen oxides ( $\text{NO}_X = \text{NO} + \text{NO}_2$ ) in the atmosphere and one of the major ions preserved in Antarctic snow and ice. Therefore, there has been great interest in using concentration and isotopic signature of nitrate in ice cores to reconstruct past atmospheric  $\text{NO}_X$  sources and their oxidation processes to nitrate. For interpretation of nitrate records in Antarctic ice cores, it is necessary to know the long-term changes of concentration and isotopic compositions ( $^{15}\text{N}/^{14}\text{N}$ ,  $^{17}\text{O}/^{16}\text{O}$  and  $^{18}\text{O}/^{16}\text{O}$ ) of nitrate in the atmosphere which deposits on the surface snow. In this study, we present seasonal variation of nitrogen and triple oxygen isotopic composition of nitrate collected at French Antarctic Station Dumont d'Urville (66°40'S, 140°01'E) throughout the year 2011. The significant increase of nitrate concentration during spring and summer period was observed and  $^{15}\text{N}$  were depleted in the nitrates, indicating that there was the substantial  $\text{NO}_X$  input to the atmosphere by photolysis of nitrate in the surface snow. In addition, relatively low  $^{17}\text{O}$  excess in summer period suggests that  $\text{NO}_X$  oxidation to nitrate by OH radicals was increased. On the other hand, high  $^{17}\text{O}$  excess with low concentration in fall and winter period suggests that OH oxidation pathway was depleted and other oxidation pathways related to  $\text{O}_3$  were dominant. Additionally, the small nitrate increase in winter period might be attributed to the transport of stratospheric nitrate to troposphere due to the formation of polar stratospheric clouds. In the presentation, we will discuss the long-term change of the seasonal trends and compare the result with that of 2001 year-round isotopic analysis using nitrate aerosols at the same station.

Keywords: Antarctic, Aerosol, Nitrate, Stable isotopic analysis

## Determination on the triple oxygen isotopic composition of atmospheric nitrous acid (HONO)

NAKANE, Ray<sup>1\*</sup>; OHYAMA, Takuya<sup>1</sup>; NAKAGAWA, Fumiko<sup>1</sup>; TSUNOGAI, Urumu<sup>1</sup>; NOGUCHI, Izumi<sup>2</sup>; YAMAGUCHI, Takashi<sup>2</sup>

<sup>1</sup>Graduate School of Environmental Studies, Nagoya University, <sup>2</sup>Hokkaido Institute of Environmental Sciences

The photolysis of nitrous acid (HONO) has been recognized as a potentially important source of OH radicals, which is known as a major oxidant in the atmosphere removing reductive trace gases such as methane and NMHCs. There are two major formation pathways to produce atmospheric HONO, one is a process so-called “direct emission” in which HONO emits directly from various sources on the ground and the other “secondary formation” in which HONO is produced by chemical reaction of nitrogen compounds in the atmosphere. Their contributions to the production of atmospheric HONO, however, have not been well understood.

In order to quantify the contribution of HONO derived from secondary formation, we determined a triple oxygen isotope,  $\Delta^{17}\text{O}$  value of atmospheric nitrous acid (HONO).  $\Delta^{17}\text{O}$  value of HONO produced via secondary formation is expected to have highly positive values as those of  $\text{O}_3$  ( $\Delta^{17}\text{O} = +30 \pm 10 \text{‰}$ ), while no  $\Delta^{17}\text{O}$  anomaly ( $\Delta^{17}\text{O} = 0 \text{‰}$ ) should be observed for HONO which is emitted directly from various sources on the ground.

Atmospheric HONO was collected using filter-pack method (Noguchi et al., 2007) in which HONO accumulates on the  $\text{K}_2\text{CO}_3$  impregnated filter as  $\text{NO}_2^-$ . Since HONO is collected as  $\text{NO}_2^-$ , we must be careful about oxygen exchange between  $\text{NO}_2^-$  and  $\text{H}_2\text{O}$  on the filter. If the sampling period becomes longer,  $\Delta^{17}\text{O}$  of HONO could become smaller than the original value due to rapid oxygen exchange between  $\text{NO}_2^-$  and  $\text{H}_2\text{O}$  on the filter. Therefore, in order to decide appropriate sampling periods for  $\Delta^{17}\text{O}$  measurement of HONO, we conducted a field sampling of atmospheric HONO during December 15-26, 2014, at Hokkaido Institute of Environmental Sciences, Sapporo, Japan. We arranged seven different periods (half a day, one day, two days, three days, four days, one week and two weeks) for atmospheric HONO collection. We also set two kinds of sampling flow rate for HONO sampling; faster flow rate (10 L/min) for shorter sampling periods (from half a day to three days) and slower flow rate (4 L/min) for longer sampling periods (from four days to two weeks). HONO-derived  $\text{NO}_2^-$  on the filter was extracted to pure water. After that, it was reduced to  $\text{N}_2\text{O}$  using  $\text{HN}_3$  and then converted to  $\text{O}_2$  via thermal decomposition and then introduced to IRMS for  $\Delta^{17}\text{O}$  measurement. The concentration of  $\text{NO}_2^-$  and  $\text{NO}_3^-$  in the extracted water were measured by traditional ion chromatography to calculate  $\text{NO}_2^-$  yield (ratio of  $\text{NO}_2^-$  among the sum of  $\text{NO}_2^-$  and  $\text{NO}_3^-$ ) on the filter.

We found clear difference on  $\text{NO}_2^-$  yield absorbed on the filter between the two sample flow rates. Low flow rate (4 L/min) result in lower  $\text{NO}_2^-$  yield of around 79% on average which coincide well with those reported previously (76%, Ohyama et al., 2012). Very high  $\text{NO}_2^-$  yield of more than 98% were observed in the filter collected at high rates (10 L/min). We concluded that we could prevent  $\text{NO}_3^-$  formation via reaction of  $\text{NO}_2^-$  with  $\text{O}_3$  by collecting HONO in the condition of higher sample flow rate.

The result of  $\Delta^{17}\text{O}$  value of HONO ranged from +6 ‰ to +9 ‰ through the observation periods. We could not find any  $\Delta^{17}\text{O}$  depletion due to oxygen exchange between  $\text{NO}_2^-$  and  $\text{H}_2\text{O}$  on the filter during the collection periods. Assuming that  $\Delta^{17}\text{O}$  value of HONO derived from secondary formation is +35 ‰, the contribution of HONO produced via secondary formation to atmospheric HONO was estimated to be about more than 20% demonstrating its significance on the formation pathway of atmospheric HONO in the winter of urban area.

Keywords: HONO, nitrous acid, triple oxygen isotope, source, winter, Sapporo

## Determination of partitioning of alpha-pinene ozonolysis products between gaseous and aerosol phases

INOMATA, Satoshi<sup>1\*</sup> ; TANIMOTO, Hiroshi<sup>1</sup> ; SATO, Kei<sup>1</sup> ; FUJITANI, Yuji<sup>1</sup> ; YAJIMA, Ryoji<sup>2</sup> ;  
SAKAMOTO, Yosuke<sup>2</sup> ; HIROKAWA, Jun<sup>2</sup>

<sup>1</sup>National Institute for Environmental Studies, <sup>2</sup>Hokkaido University

Organic material accounts for a substantial fraction of atmospheric fine particulate matter, which directly and indirectly affects the global climate as well as human health. Many gas-phase organic compounds undergo oxidation in the gas phase to yield products, generally oxygenated, that have vapor pressures sufficiently low that they are partitioned between the gas and aerosol phases. Such compounds are often referred to as semi-volatile organic compounds (SVOCs) and, when present in the aerosol phase, as secondary organic aerosols (SOAs). Quantification of the impacts of SOAs requires understanding their chemical composition and processes of formation as well as mass yields. In particular, because a systematic underestimation of simulated SOA production increases with air mass ageing, speciation of the SVOCs produced by gaseous oxidation is essential. In addition, information about the partitioning of each SVOC between the gaseous and condensed phases as well as the reactions of the condensed SVOCs within the particulate phase is important for the description of SOA formation. We use chemical ionization-mass spectrometry to identify SVOCs in both the gaseous and the aerosol phases and to estimate the gas-aerosol partitioning of each SVOC. By using the same technique to measure SVOCs in both the gaseous and the aerosol phases, we were able to determine the partitioning of each SVOC between the gaseous and aerosol phases from the ratio of ion signals, without knowing the concentration of each SVOC. This ability to partition each SVOC between the gaseous and aerosol phases is a strong point of this approach, because most chemical species in SOAs are thought to be multifunctional, and determining their concentrations seems to be impossible. In the present study, we used two proton transfer reaction-mass spectrometers for real-time measurements of SVOCs produced in  $\alpha$ -pinene ozonolysis in both the gaseous and the aerosol phases and determined the partitioning of each SVOC between the gaseous and aerosol phases. Time profiles of the SVOCs in both the gaseous and the aerosol phases were compared. This work was supported by the Environmental Research and Technology Development Fund (5-1408) of the Ministry of the Environment, Japan.

Keywords: Secondary organic aerosol, Gas-particle partitioning, Chemical ionization-mass spectrometry, Proton transfer reaction-mass spectrometry, alpha-Pinene, Ozonolysis

## Impact of oxidation processes on optical properties of isoprene SOAs

NAKAYAMA, Tomoki<sup>1\*</sup> ; SATO, Kei<sup>2</sup> ; IMAMURA, Takashi<sup>2</sup> ; MATSUMI, Yutaka<sup>1</sup>

<sup>1</sup>Solar-Terrestrial Environment Laboratory, Nagoya University, <sup>2</sup>National Institute for Environmental Studies

Isoprene is the most abundant volatile organic compounds (VOCs) emitted from biosphere and is known as one of the precursors of secondary organic aerosols (SOAs) in the atmosphere. The formation yield of the isoprene-SOAs is considered to be enhanced in the presence of acidic seed particles such as sulfuric acid. Recently, it has been suggested that some organic aerosols, which is called "brown carbon", can absorb solar radiation, especially at the ultraviolet (UV) and shorter visible wavelengths and contribute to the radiation balance and photochemical reactions in the atmosphere. However, no experimental study on complex refractive index (RI) of the SOAs generated from the isoprene has been reported. In this work, wavelength dependence of the complex RI values of the SOAs generated in the oxidation of isoprene with OH, NO<sub>3</sub>, and O<sub>3</sub> in the presence or absence of SO<sub>2</sub> have been examined.

The SOAs were generated in a 6 m<sup>3</sup> Teflon coated stainless steel photochemical smog chamber. In the OH oxidation experiments, the reaction mixture of isoprene and NO in the presence or absence of SO<sub>2</sub> (sulfuric acid precursor) was continuously irradiated by UV light after the addition of a small amount of methyl nitrite as a source of OH radicals. In the ozonolysis experiments, isoprene was reacted with O<sub>3</sub> in the presence or absence of CO (OH scavenger) and SO<sub>2</sub>. In the NO<sub>3</sub> oxidation experiments, ozone was added to the mixture of isoprene and NO<sub>2</sub> in the presence of SO<sub>2</sub>. The optical properties of the SOAs were measured by two photoacoustic spectrometers (PASS-3 and PAX, absorption and scattering at 375, 405, 532, 781 nm) and a custom-built cavity ring-down spectrometer (CRDS, extinction at 532 nm). Chemical properties of aerosols were also measured by an Aerodyne aerosol mass spectrometer (ToF-AMS). The size distributions of SOAs were measured by a scanning mobility particle sizer (SMPS).

Absorption, scattering, and extinction efficiencies of SOAs are calculated by dividing the absorption, scattering, and extinction coefficients by total mobility cross sections measured with the SMPS. The RI of the SOAs is determined by comparing the size parameter dependence of extinction, scattering, and absorption efficiencies with Mie theory. The significant imaginary part values of RI at 405 and 532 nm are obtained for the SOAs generated in the OH oxidation of isoprene in the presence of SO<sub>2</sub>, while the imaginary part values are negligible for the SOAs generated in the ozonolysis (in the presence of OH scavenger) and NO<sub>3</sub> oxidation of isoprene. In the presentation, relationship with chemical properties and the atmospheric implications of the results will also be discussed.

Keywords: Isoprene, Secondary organic aerosol, Aerosol optical properties, Complex refractive index, Brown carbon

## Effects of relative humidity on tetrol formation from isoprene/NO photo-oxidation

SATO, Kei<sup>1\*</sup> ; OKUMURA, Motonori<sup>2</sup> ; TAKAMI, Akinori<sup>1</sup> ; IMAMURA, Takashi<sup>1</sup>

<sup>1</sup>National Institute for Environmental Studies, <sup>2</sup>Kyoto University

2-Methyltetrols, molecular markers of isoprene secondary aerosol, are produced by the particle-phase hydrolysis of organonitrate esters (Sato, 2008; Szmigielski *et al.*, 2010; Jacobs *et al.*, 2014) and/or the particle-phase oxidation of isoprene epoxydiols (Jacobs *et al.*, 2014) during the isoprene/NO<sub>x</sub> photo-oxidation. The effects of relative humidity, acid and base on 2-methyltetrol formation from the isoprene/NO photo-oxidation were investigated. We used a 6-m<sup>3</sup> Teflon bag and a 6-m<sup>3</sup> stainless steel chamber for humid and dry conditions, respectively. 2-Methyltetrol formation under humid conditions (RH  $\simeq$  80%) was enhanced in the presence of sulfur dioxide and was also enhanced in the presence of ammonia. In contrast, 2-methyltetrol formation under dry conditions (RH < 1%) was less catalyzed or suppressed in the presence of sulfur dioxide. The ratio of total 2-methyltetrol mass to total organic aerosol mass was 0.21 – 18 wt% under various present conditions. 2-Methyltetrol formation in the aqueous solution of aerosol sample was also investigated, and was found to be enhanced by both the acid and the base. The present results show that the presence of water is critical for acid-catalyzed 2-methyltetrol formation from isoprene/NO photo-oxidation. The ester hydrolysis will be a major pathway for 2-methyltetrol formation because it was enhanced by the base.

This work was supported by a Grant-in-Aid for Scientific Research from the Japan Society for the Promotion of Science (No. 25340021, FY2013 – 2015). K.S. and M.O. thank Professor Susumu Tohno of Kyoto University for supplying a GC/MS instrument.

References: Sato, K. (2008) *Atmos. Environ.* **42**, 6851 – 6861. Szmigielski, R. *et al.* (2010) *Atmos. Res.* **98**, 183 – 189. Jacobs, M. I. *et al.* (2014) *Atmos. Chem. Phys.* **14**, 8933 – 8946.

Keywords: biogenic volatile organic compound, secondary organic aerosol, organic nitrate, aqueous-phase reaction, environmental chamber



## Continuous observations of atmospheric HCHO by MAX-DOAS at Yokosuka, Japan: Verification and correlation with ozone

KANAYA, Yugo<sup>1\*</sup> ; POSTYLYAKOV, Oleg<sup>2</sup> ; IRIE, Hitoshi<sup>3</sup> ; TAKASHIMA, Hisahiro<sup>4</sup>

<sup>1</sup>DEGCR/JAMSTEC, <sup>2</sup>Institute of Atmospheric Physics, Russian Academy of Sciences, <sup>3</sup>Chiba University, <sup>4</sup>Fukuoka University

Tropospheric ozone is an important greenhouse gas with the third largest global warming effect after CO<sub>2</sub> and CH<sub>4</sub>. Its photochemical production in the atmosphere is not quantitatively understood, partly because of the large uncertainties in the amount and origins of the volatile organic compounds (VOCs) in the atmosphere serving as precursors of ozone. Accurate observations of formaldehyde (HCHO), formed from VOC oxidation simultaneously with ozone, would provide pivotal information of the VOC emission rates and ozone production mechanisms. This study focuses on the measurements of HCHO in the urban area, specifically at Yokosuka (35.32 degN, 139.65 degE), Japan. Appropriateness of the observations was verified and then the correlation with ozone concentrations was studied.

Differential slant column densities of HCHO were derived from MAX-DOAS spectrum observations (336.5 - 359 nm) at Yokosuka and then converted to the vertical column densities/profiles using aerosol information retrieved simultaneously. We obtained observational data from October 2007 to December 2013, and from 08H (0800-0900 JST) to 15H in winter and from 06H to 17H in summer. The HCHO concentrations at the lowest layer derived from MAX-DOAS agreed quite well with the monthly ground-based observations of HCHO conducted at Oppama site, 2 km west of our location. Although we showed that recent satellite observations of HCHO provided reasonable agreement with MAX-DOAS over a rural site near Moscow, Russia, poorer agreement was obtained at Yokosuka, potentially affected by the spatial inhomogeneity in the HCHO concentrations in or near the urban region.

Monthly averages of the tropospheric vertical column density of HCHO derived from MAX-DOAS at 13H showed clear seasonal variation with maxima during July-September ( $(1.4-2.0) \times 10^{16}$  molecules cm<sup>-2</sup>) and minima during December-March. The temporal variation during summer was quite similar to that of ozone concentrations observed at Oppama, while the HCHO levels were quite low in April/May, when the ozone concentration was even higher. The HCHO partial column in the lowest 1 km altitude range at 13H during June-August showed tight positive correlation with the surface ozone concentrations. These analyses suggested that the MAX-DOAS observations of HCHO are successful in quantifying HCHO secondarily produced in the atmosphere by photochemistry and that the short-lived HCHO would be a useful tracer to differentiate in-situ ozone production from long range transport.

Keywords: Tropospheric photochemistry, Volatile organic compounds, Urban atmosphere, Ozone precursors

## Evaporation of aerosol particles upon heating in a transmission electron microscope

ADACHI, Kouji<sup>1\*</sup>

<sup>1</sup>Meteorological Research Institute

Thermal property (e.g., evaporation temperature) of atmospheric aerosol particles is important to measure and classify their species using, for example, an aerosol mass spectrometer, a thermos denuder, and thermal method for elemental carbon/organic carbon (EC/OC). However, it is largely unknown about the thermal behavior of ambient aerosol particles especially organic aerosol particles and their mixture with inorganic materials. Therefore, evaporation temperatures of ambient aerosol particles with their compositions need to be determined.

This study uses a transmission electron microscope (TEM) and a heating holder, which can heat samples on TEM grids >1000 °C while observing their shapes. Thus, it is possible to observe particle evaporation process upon heating. The TEM chamber is in vacuum (~0.00001Pa) and lacks of oxygen. Thus, particle volumes on TEM grids changes through evaporation/sublimation at specific temperature. In general, an aerosol mass spectrometer uses 600 °C to vaporize aerosol particles, a thermos denuder uses 200-300 °C to remove volatile materials, and an EC/OC measurement use ~500 °C to distinguish OC and EC. Thus aerosol thermal properties were analyzed by heating from room temperature to 600 °C.

This study mainly used ambient samples collected from biomass burning during Biomass Burn Observation Project (BBOP) in 2013. These samples were collected at North America using an aircraft. The results indicated that organic materials in biomass burning lost their volume while heating up to 600 °C but did not completely evaporate but remained residue, which is probably due to charring of organic matters. Especially, spherical brown carbon organic particles occurring in biomass burning (tar balls) left their volume by 30% at 600 °C. The results imply that tar balls are difficult to measure their properties when assuming they are volatile materials even at 600 °C.

Acknowledgements: The author acknowledges the BBOP campaign team, especially L I Kleinman, A, J Sedlacek, and P R Buseck, for their helps for the sampling and the analyses of BBOP samples.

Keywords: aerosol, heating, organic matter, transmission electron microscopy, biomass burning

## Speciation of sulfate in aerosols for the precise estimation of its global cooling effect

MIYAMOTO, Chihiro<sup>1\*</sup>; YAMAKAWA, Yoshiaki<sup>1</sup>; SAKATA, Kohei<sup>2</sup>; MIYAHARA, Aya<sup>2</sup>; SUGA, Hiroki<sup>2</sup>; SAKAGUCHI, Aya<sup>3</sup>; TAKEICHI, Yasuo<sup>4</sup>; ONO, Kanta<sup>4</sup>; TAKAHASHI, Yoshio<sup>1</sup>

<sup>1</sup>Department of Earth and Planetary Science, Graduate School of Science, The University of Tokyo, <sup>2</sup>Department of Earth and Planetary Systems Science, Graduate School of Science, Hiroshima University, <sup>3</sup>Faculty of Pure and Applied Science, University of Tsukuba, <sup>4</sup>Institute of Materials Structure Science, KEK

Global cooling effect by aerosol is one of causes which influence earth's climatic change (IPCC, 2013). In particular, sulfate aerosols are known to cool the earth indirectly by forming cloud condensation nuclei (CCN) because of their high hygroscopicity. However, the hygroscopicity can change depending on the sulfate species. For example,  $\text{CaSO}_4 \cdot 2\text{H}_2\text{O}$  is sulfate having low hygroscopicity. Therefore, determination of sulfate species in aerosols is necessary to interpret the degree of cooling effect by sulfate aerosols in environment.

In this study, aerosol sampling was conducted in Higashi-Hiroshima (34.40 N, 123.71 E), Hiroshima, Japan. In addition, the samples were collected using two methods as to particle size. One method collected non-size-fractionated aerosols for about a year from September 2012 to September 2013. The other method collected size-fractionated aerosol in various periods such as winter when concentrations of anthropogenic aerosols were high (PA sample; collected from January 31 to February 1, 2013), spring (March 4 to 9, 2013), summer (July 22 to August 5, 2013), and fall (November 11 to 25, 2013). For these samples, major ion composition was measured by ion-chromatography, while chemical species of sulfur and calcium in the aerosol samples were determined by X-ray absorption fine structure (XAFS) spectroscopy. Furthermore, to unravel the function of CCN by sulfate aerosols in more detail, samples for single particle analysis were collected on May 31, 2014 during a dust event, which was analyzed individually using scanning transmission X-ray microscopy (STXM).

Atmospheric concentration of each major ion in the atmosphere had seasonal variation. Sulfate ion ( $\text{SO}_4^{2-}$ ) concentration was larger in PA, in which concentration of ammonium ion ( $\text{NH}_4^+$ ) and nitrate ion ( $\text{NO}_3^-$ ) were also larger than those in other seasons. Meanwhile, size distribution of aerosol is important to determine its origin, because it is widely recognized that aerosol larger than  $1 \mu\text{m}$  diameter is of natural origin. On the other hand, particles finer than  $1 \mu\text{m}$  is of anthropogenic origin. In general, concentrations of  $\text{SO}_4^{2-}$  and  $\text{NH}_4^+$  were larger in finer particles. Therefore, it is strongly suggested that the aerosol sample collected in this period was influenced by human activities. In spring, concentration of calcium ion ( $\text{Ca}^{2+}$ ) increased particularly in the coarse particles, which suggests that its origin was from natural source.

Subsequently, sulfate species in the aerosol samples was determined using XAFS, where it was found that concentration ratio of calcium sulfate ( $\text{CaSO}_4 \cdot 2\text{H}_2\text{O}$ ) which has low hygroscopicity to total concentration of  $\text{SO}_4^{2-}$  in the aerosol sample ( $[\text{CaSO}_4 \cdot 2\text{H}_2\text{O}]/[\text{SO}_4^{2-}]_t$ ) was larger in spring than that in PA. The abundance of  $\text{CaSO}_4 \cdot 2\text{H}_2\text{O}$  in atmosphere cannot be ignored because of its comparatively high  $[\text{CaSO}_4 \cdot 2\text{H}_2\text{O}]/[\text{SO}_4^{2-}]_t$  ratio, especially in spring. It was also found that indirect cooling effect by sulfate will be small in spring due to the larger ratio of  $[\text{CaSO}_4 \cdot 2\text{H}_2\text{O}]/[\text{SO}_4^{2-}]_t$ . To provide further details of the effect by CCN function, Ca species of single particle samples in the dust period was determined using STXM. It was shown that there was  $\text{CaSO}_4 \cdot 2\text{H}_2\text{O}$  at the surface of the particle, which is the site of the chemical reactions with other species in aerosols. In addition,  $\text{Ca}(\text{NO}_3)_2 \cdot 4\text{H}_2\text{O}$ , which was minor Ca species in the bulk analysis, was also detected in the particles. Individual analysis of single particle is important to determine minor species in aerosol samples, which leads to better understanding of chemical processes in the atmosphere.

In conclusion, it was suggested that the degree of indirect cooling effects of sulfate aerosol can change seasonally because concentrations of low hygroscopicity sulfate species in the atmosphere are variable.

Keywords: aerosol, speciation of sulfate, global cooling effect, X-ray absorption fine structure

## Interaction between oxalate aerosol and metal: stability and global cooling effect of aerosol

YAMAKAWA, Yoshiaki<sup>1\*</sup> ; SAKATA, Kohei<sup>2</sup> ; MIYAHARA, Aya<sup>2</sup> ; MIYAMOTO, Chihiro<sup>2</sup> ; TAKAHASHI, Yoshio<sup>1</sup> ; SAKAGUCHI, Aya<sup>3</sup>

<sup>1</sup>University of Tokyo, <sup>2</sup>Hiroshima University, <sup>3</sup>University of Tsukuba

Photoreaction contributes to the formation and removal processes of oxalic acid that is a major component of organic aerosols. Oxalic acid is formed by photooxidation of high molecular weight organic aerosols via glyoxylic acid, and decomposed into carbon dioxide. In addition, previous study showed that oxalic acid forms insoluble metal-oxalate complex, which suggested that global cooling effect of oxalic acid is lower than previous estimation because metal-oxalate complex does not work as cloud condensation nuclei. Interaction between oxalic acid and metal might affect photoreactivity like hygroscopicity. In this study, speciation of oxalic acid and measurement of reaction rate constant for photoreaction were conducted to evaluate the effect of metal for global cooling effect and photoreaction.

Size fractionated aerosol samples were collected at Higashi-Hiroshima in winter, spring, and summer. Speciation analysis of oxalic acid was conducted by X-ray absorption fine structure (XAFS) spectroscopy for zinc (Zn), lead (Pb), and Calcium (Ca). Photoreaction experiments were conducted by ultraviolet ray about oxalic acid and glyoxylic acid. Oxalic acid and glyoxylic acid were measured by Total Organic Carbon (TOC) Analyzer and colorimeter using Schiff base, respectively.

As a result of speciation, Ca and Zn oxalate complexes were found in fine particles ( $<1.7 \mu\text{m}$ ), but Pb complex was hardly found. The ratio of metal-oxalate complexes to total oxalic acid was about 30% to 50% about each sample. This result showed that the cooling effect of oxalic acid might be smaller than previous estimation.

As a result of photolysis experiments, half-life time of oxalic acid, Mg complex, and Zn complex is 19 minutes, 71 minutes, and 172 minutes, respectively. This result showed that photoreactivity of oxalic acid was decreased due to the decrease of quantum yield by forming metal-oxalate complexes. In contrast, photoreactivity of glyoxylic acid was increased by coexisting with Zn. Photoreaction of glyoxylic acid to oxalic acid is addition reaction of oxygen, which differs that of oxalic acid to carbon dioxide by cutting carbon bond. It is thought that the reason why photoreactivity was improved is what Zn worked as catalyst.

Keywords: organic aerosol, oxalic acid, metal complex, photo reactivity, indirect effect

## Major ion composition in aerosol: As an new indicator of chlorine deficiency

SAKATA, Kohei<sup>1\*</sup>; SAKAGUCHI, Aya<sup>2</sup>; TAMENORI, Yusuke<sup>3</sup>; OGAWA, Masahiro<sup>4</sup>; TAKAHASHI, Yoshio<sup>5</sup>

<sup>1</sup>Earth and Planetary Systems Science, Graduate School of Science, Hiroshima University, <sup>2</sup>Faculty of Pure and Applied Science, University of Tsukuba, <sup>3</sup>Japan Synchrotron Radiation Research Institute (JASRI), <sup>4</sup>SR-center Ritsumeikan University, <sup>5</sup>Department of Earth and Planetary Science, Graduate School of Science, The University of Tokyo

A large part of sodium and chlorine in aerosol particles are derived from surface seawater as sodium chloride (sea-salt; NaCl). Sodium chloride in aerosol is altered to sodium nitrate (NaNO<sub>3</sub>) and sulfate (Na<sub>2</sub>SO<sub>4</sub>) by the reaction with nitric acid (HNO<sub>3</sub>) and sulfuric acid (H<sub>2</sub>SO<sub>4</sub>) in atmosphere, respectively. In these reactions, gaseous HCl is emitted from sea-salt particles to the atmosphere, which is called as chlorine deficiency. These are important chemical reactions to anthropogenic N, in the process of transport from continent to open ocean, and to H<sub>2</sub>SO<sub>4</sub> as scavenging process in atmosphere (Akimoto, 2014). However, detail processes of the chemical reaction and size-dependence of aerosol particles on this reaction are not clear. In order to clarify these reactions/processes in aerosol, we employed mass fractions (MF) parameter to size-fractionated aerosol particles obtained from land/continent and ocean. Direct speciation of Na was also conducted by soft X-ray absorption fine structure (XAFS) spectroscopy to intercompare the abundance ratio of Na species to those estimated by MF.

Size-fractionated aerosol particles on land were collected by a high volume cascade impactor at Higashi-Hiroshima from December 2012 to March 2014. Marine total suspended particulate (TSP) and size-fractionated aerosol particles were collected in the *R/V Hakuho-Maru* research cruises of KH-12-4 (the North Pacific Ocean: from 23th August to 3rd October 2012) and KH-13-4 Leg. 4 (the Bay of Bengal: from 31th July to 14th August 2013), respectively. Major ionic concentrations (Na<sup>+</sup>, NH<sub>4</sub><sup>+</sup>, K<sup>+</sup>, Mg<sup>2+</sup>, Ca<sup>2+</sup>, Cl<sup>-</sup>, NO<sub>3</sub><sup>-</sup> and SO<sub>4</sub><sup>2-</sup>) in aerosol samples were determined by an ion chromatography after appropriate pretreatment. MF parameters were calculated as  $[X]_{eq}/[\text{total anion}]_{eq}$  (X: Cl<sup>-</sup>, NO<sub>3</sub><sup>-</sup> and nssSO<sub>4</sub><sup>2-</sup>). Direct speciation of Na in continental size-fractionated aerosol particles were conducted by XAFS spectroscopy on BL-10, SR-center, Ritsumeikan University.

MF[Cl<sup>-</sup>]<sub>eq</sub> was inversely correlated with both MF[NO<sub>3</sub><sup>-</sup>]<sub>eq</sub> and MF[nssSO<sub>4</sub><sup>2-</sup>]<sub>eq</sub> in continental coarse aerosol particles. It can be said that the chlorine deficiency is explained by the reaction with NO<sub>3</sub><sup>-</sup> and/or nssSO<sub>4</sub><sup>2-</sup>. The regression line for MF[Cl<sup>-</sup>]<sub>eq</sub>-MF[nssSO<sub>4</sub><sup>2-</sup>]<sub>eq</sub> was -2.16. As for MF[Cl<sup>-</sup>]<sub>eq</sub>-MF[NO<sub>3</sub><sup>-</sup>]<sub>eq</sub>, the regression line shows -1.03, and this regression line satisfies the equation of y=1-x. Thus, HNO<sub>3</sub> has large contribution as a reactant of NaCl in the urban atmosphere. Furthermore, chemical reaction of NaCl with HNO<sub>3</sub> and H<sub>2</sub>SO<sub>4</sub> preferentially occur on the small aerosol particles because further decrement of MF[Cl<sup>-</sup>]<sub>eq</sub> was found in smaller size of aerosols compared with that of large aerosol particles. The speciation analysis with XAFS spectroscopy showed comparable results with that obtained from MF analysis using the high reacted aerosol samples from continent (MF[Cl<sup>-</sup>]<sub>eq</sub> : MF[NO<sub>3</sub><sup>-</sup>]<sub>eq</sub> : MF[nssSO<sub>4</sub><sup>2-</sup>]<sub>eq</sub> =18:56:23). As for marine aerosol samples from the North Pacific Ocean, dominant reactant of NaCl is H<sub>2</sub>SO<sub>4</sub>. On the other hand, the reaction of NaCl occurs with both NO<sub>3</sub><sup>-</sup> and SO<sub>4</sub><sup>2-</sup> above the Bay of Bengal.

As a consequence, MF is very useful tools to find dominant reactant of NaCl and Na chemical species as a result of chlorine deficiency in both continental and marine aerosol particles.

Keywords: atmospheric chemistry, aerosol, Na, XAFS spectroscopy

## Coating of black carbon aerosols and increase of their light absorption coefficient observed in Tokyo

AOKI, Haruki<sup>1\*</sup> ; KITA, Kazuyuki<sup>2</sup> ; MOTEGI, Nobuhiro<sup>3</sup> ; OHATA, Sho<sup>3</sup> ; ADACHI, Kouji<sup>4</sup> ;  
IGARASHI, Yasuhito<sup>4</sup> ; KOIKE, Makoto<sup>3</sup> ; KONDO, Yutaka<sup>3</sup>

<sup>1</sup>Graduate School of Science and Engineering, Ibaraki University, <sup>2</sup>College of Science, Ibaraki University, <sup>3</sup>Graduate School of Science, The University of Tokyo, <sup>4</sup>Meteorological Research Institute

Black carbon (BC) aerosols can influence the climate due to the heating the atmosphere by their strong light absorption (direct effect). Light absorption coefficient of BC is varied with their size, shape and mixing states. BC is often coated with other aerosol component such as organics and sulfate, and the coating is supposed to cause the increase of light absorption coefficient (lens effect). Lens effect has still not fully understood because the coating material and amount in the real atmosphere have not understood quantitatively. Therefore it is important to observe change of light absorption coefficient of BC and their shape and mixing state simultaneously. Our group conducted intensive observation of various parameters of BC, including light absorption coefficient and coating amount, in huge city, Tokyo. In this paper, variation of light absorption coefficient of BC in Tokyo and its relation with BC coating is studied.

Intensive BC observation named as Black Carbon / Carbonaceous Aerosol Removal Experiment (BC-CARE) were conducted from July 28 to August 15 in 2014. The atmospheric BC was sampled and observed at the sixth floor (20m) in Tokyo University, located central Tokyo city area. Light absorption coefficient was measured using the photoacoustic soot spectrometer (PASS). Amplification factor (FA) by coating of BC was evaluated from the ratio of light absorption coefficient in the unheated sampled air to that in the 300 °C heated air, where volatile coating materials were removed from BC. BC mass concentration and the ratio of coating thickness with BC diameter (Dp/Dc) was measured using single-particle soot photometer (SP2) simultaneously. During observation period, aerosol particle were regularly sampled and the BC size, shape and mixing states were observed using a transmission electron microscope (TEM).

The significant increase in BC light absorption coefficient with the BC coating was measured on 29th July. Maximum increase was about 80% in this period. In the early half of this period, FA and Dp/Dc values were increased correlatingly from about 1.0 to about 1.8. However, in the latter half of this period, FA values were gradually decreased although Dp/Dc values kept high. Observation with TEM showed that many coating BC particles larger than 1 $\mu$ m in the early half of this period. In the latter half, particle size of coated BC was generally less than 0.5 $\mu$ m. Because the measuring range of particle size of SP2 is less than 1 $\mu$ m and PASS can measure BC about 1 $\mu$ m or more, the difference between the two period may be cause by the contribution of these larger BC particles. However, both PASS and SP2 can measure BC particles less than 0.5 $\mu$ m, these results cannot fully explain the observed difference in FA and Dp/Dc behavior.

Keywords: Black carbon, Light absorption coefficient, Lens effect, Electron microscope

## Online Measurement of Aerosol Chemical Composition Classified by Black Carbon Mixing State using a LII-MS

OZAWA, Yuya<sup>1\*</sup> ; TAKEDA, Naoki<sup>2</sup> ; KOIZUMI, Kazuhiro<sup>2</sup> ; TAKEGAWA, Nobuyuki<sup>3</sup>

<sup>1</sup>The University of Tokyo, <sup>2</sup>Fuji Electric, Co., Ltd., <sup>3</sup>Tokyo Metropolitan University

Aerosols have large influences on the radiation budget of the Earth's atmosphere by scattering or absorbing solar visible radiation (direct effect) and by altering cloud microphysical properties (indirect effect) (IPCC, 2013). These effects can significantly depend on the chemical composition and mixing state of aerosol particles. Specifically, the mixing state of sulfate, nitrate, and organics with black carbon (BC) is a key parameter for estimating the aerosol direct and indirect effects.

We have developed a new method to measure aerosol chemical composition classified by the mixing state with BC by combining laser induced incandescence (LII) and mass spectrometric (MS) methods (LII-MS, Miyakawa et al., AST, 48, 853-863, 2014). The purpose of this study is to further evaluate the LII-MS in the laboratory and also to understand the temporal variations of BC mixing state in a suburban area in Tokyo.

The LII-MS consists of a series of LII and MS. In the LII section, BC containing particles introduced into a near-infrared laser cavity can be efficiently vaporized and incandescence signals from the BC particles are detected. The sample air is then introduced into the MS section by a tandem nozzle to measure the mass concentrations of sulfate and nitrate (Takegawa et al., AST, 46, 428-443, 2012). The aerosol composition classified by the BC mixing state is obtained by alternatively switching on and off the LII laser.

Several modifications of the LII-MS hardware and additional experiments have been performed compared to the previous version presented by Miyakawa et al. (2014). First, the control electronics for switching the LII laser has been modified to achieve more stable operation. Second, the cycle of the LII laser on/off and zero-air modes has been modified to improve the quantification of the BC mixing state. Third, the performance of the tandem nozzle, which is one of the key components of the LII-MS, has been tested in the laboratory to investigate the stability and reproducibility of the particle transport efficiency. Ambient measurements have been conducted at the Tokyo Metropolitan University to test the overall performance of the LII-MS and to investigate the temporal variation of the BC mixing state in suburban air. Details of the laboratory experiments and ambient measurements will be presented and discussed.

Keywords: Aerosol, BC mixing state, Laser-induced incandescence, Mass spectrometer

## Single-particle measurement of iron-containing dust particles using a laser-induced incandescence technique

YOSHIDA, Atsushi<sup>1\*</sup> ; MOTOKI, Nobuhiro<sup>1</sup>

<sup>1</sup>Graduate School of Science, The University of Tokyo

### 1. Introduction

Two major light-absorbing ubiquitous in earth atmosphere, black carbon (BC) and mineral dust, contribute positive climate forcing by absorbing solar radiation in atmosphere and by reducing albedo of snowpack. Light-absorption efficiency of mineral dust has shown to be strongly correlated with iron-content [Moosmueller 2012]. Reliable data for concentration and micro-physical properties (size distribution, mixing state, complex refractive index, etc.) of BC and iron-containing dust particles are important to provide a physical basis in climate simulations.

For statistical sampling and continual observations, we need a fast and real-time technique to measure concentrations and the microphysical properties of these light-absorbing particles. In this study, we experimentally show that the laser-induced incandescence (LII) technique, which has been used only for BC measurement so far, is also effective for identifying and measuring iron-containing dust particles.

### 2. Laser-induced incandescence (LII)

We use the single-particle soot photometer (SP2, Droplet measurement technology) to measure laser-induced incandescence and light-scattering signals for individual particles. In SP2, sample air containing aerosols are continually introduced into an intra-cavity Nd:YAG laser beam with 1064 wavelength. Refractory light-absorbing particles with boiling higher than  $\sim 3000\text{K}$  emit thermal radiation detectable in visible wavelength. In SP2, thermal radiation is measured at two distinct wavelength bands, the blue-band (300-500 nm) and the red-band (580-710 nm), to infer the spectra of incandescent light. As the spectra of thermal radiation shifts shorter wavelength as temperature increases, the blue-band to red-band signal ratio (color ratio) is a proxy of boiling point of the incandescing particle.

### 3. Identification of incandescing particles

The probability distribution of measured color ratio for various laboratory samples and field dust samples are shown in Figure. For laboratory sample, there are three distinct modes in color ratio distribution: iron and iron oxides ( $\sim 1.5$ ), titanium ( $\sim 2.0$ ), and fullerene soot ( $\sim 2.6$ ) (standard material of BC). Therefore, we can distinguish incandescent materials (iron, iron oxides, titanium, BC) in a particle using the value of color ratio.

Figure also shows the result for two field samples: Iceland particle (provided by Dr. P. Dagsson-Waldhauserova, University of Iceland) and Taklimakan desert particle (provided by Dr. R. Tada (The University of Tokyo)). The color ratio distributions of these samples have two distinct modes with peaks around 1.5 and 2.6, corresponding to iron (and iron oxides) and fullerene soot, respectively. From the observed color ratio, the incandescing particles observed in the two field samples were identified as BC and iron-containing particles.

### 4. Calibration for iron measurement by LII

We have experimentally determined the relationships between blue-band signal intensity and mass of pure iron particle. This relationship was used as a calibration curve for estimating iron-content in field samples.

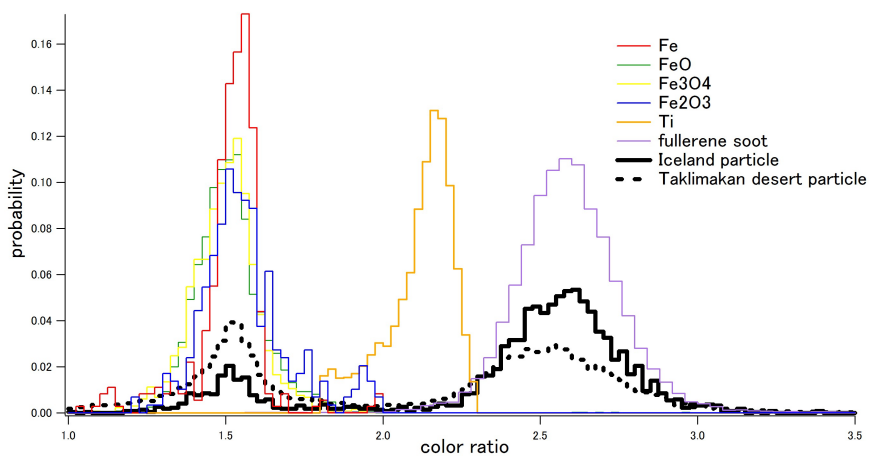
Keywords: aerosol, atmospheric chemistry



AAS21-P03

Room:Convention Hall

Time:May 27 18:15-19:30



## Development and preliminary evaluation of an aerodynamic lens for focusing nanoparticles

OTAKE, Hiroki<sup>1\*</sup> ; TAKEGAWA, Nobuyuki<sup>1</sup>

<sup>1</sup>Tokyo Metropolitan University

Aerosols have significant impacts on the radiation budget of the Earth's atmosphere by direct and indirect effects. Chemical composition of aerosol particles with diameters smaller than 100 nm (nanoparticles) is an important factor for understanding the formation process of aerosols. However, measuring chemical composition of nanoparticles is challenging because of their extremely low mass loadings in ambient air. Aerosol mass spectrometry coupled with an aerodynamic lens (ADL; Liu et al., *AST*, 22, 293, 1995), which can efficiently deliver aerosol particles into vacuum, is a useful tool for online measurements of aerosol composition. Although the concept of an aerodynamic lens for nanoparticles (nano-ADL) has been reported by previous studies (e.g., Wang et al., *IJMS*, 258, 30, 2006), the application of nano-ADL to ambient measurements has not been established. We have developed an improved nano-ADL based on the design of ADL for submicron particles (submicron-ADL) that has been used for aerosol mass spectrometry.

Laboratory experiments were performed using a custom-made particle generation system consisting of saturation and condensation tubes for oleic acid vapor. Monodisperse particles generated by a differential mobility analyzer were introduced into the submicron or nano ADL.

The detection of particles was performed using a Faraday cup. The transmission efficiency and particle beam width were measured using a movable knife-edge.

The submicron-ADL showed nearly 100% transmission efficiency for particles larger than 100 nm. On the other hand, the nano-ADL showed nearly 100% transmission efficiency at around 50 nm and decreased with increasing particle diameters, suggesting that the current design is favorable for the sampling of nanoparticles. The application of the nano-ADL to an aerosol mass spectrometry system will be discussed in the presentation.

Keywords: Aerosol, Nano particle, Aerodynamic lens, Mass spectrometry

## Evaluation of an online analysis method of nitrate aerosols using a particle trap laser desorption mass spectrometer

OIZUMI, Tomotaka<sup>1\*</sup> ; OZAWA, Yuya<sup>2</sup> ; TAKEGAWA, Nobuyuki<sup>1</sup>

<sup>1</sup>Tokyo Metropolitan University, <sup>2</sup>The University of Tokyo

Aerosols play important roles in global air quality and climate change. Ammonium nitrate, which is generated via photochemical reaction of NO<sub>x</sub>, often contributes to a major fraction of fine particles in urban air. The gas-to-particle equilibrium reaction of ammonium nitrate exhibits strong temperature dependency near ambient temperatures, which often yields evaporative loss of particles during sampling.

We have developed a particle trap-laser desorption mass spectrometer (PT-LDMS) for online measurements of aerosol chemical compositions (Takegawa et al., AST, 46, 428, 2012). Factors affecting the quantification of nitrate aerosols, including, have not been fully characterized. The purpose of this study is to evaluate the quantification of nitrate aerosols by the PT-LDMS in the current configuration and also to investigate an optimal condition for ambient sampling.

Laboratory experiments were performed by generating monodisperse ammonium nitrate particles using an atomizer and differential mobility analyzer. The dependence of the sensitivity (defined as ion signals per collected nitrate mass) on the particle trap temperature was measured by altering the temperature of the particle trap holder between 280 and 313 K. The dependence of the sensitivity on the time after particle collection until laser irradiation (exposure time) was also measured. In addition, effects of the mixing state of nitrate particles on the sensitivity were evaluated by atomizing a mixed solution of ammonium nitrate and sulfate.

Preliminary results show that the sensitivity tended to decrease with increasing the exposure time for each temperature condition, which is likely due to evaporative loss of nitrate particles in the vacuum. On the other hand, the sensitivity did not exhibit significant temperature dependency at least for the temperature conditions during the experiments.

Possible mechanisms affecting the loss of nitrate particles, along with the effects of the mixing state on the sensitivity, will be presented and discussed.

Keywords: nitrate aerosols, online analysis method, mass spectrometer

## Development of photovoltaic-driven atmospheric observation instrument Eco-MAXDOAS

KATO, Tomomichi<sup>1\*</sup> ; IRIE, Hitoshi<sup>2</sup>

<sup>1</sup>Graduate School of Advanced Integration Science, Chiba University, <sup>2</sup>Center for Environmental Remote Sensing, Chiba University

Atmospheric aerosols are an important factor controlling the Earth's climate. However, their complicated formation mechanisms and effects on climate are poorly understood. Under these circumstances, the MAX-DOAS technique that enables simultaneous measurements of aerosols and their gaseous precursors, such as nitrogen dioxide (NO<sub>2</sub>), has been developed by Chiba University. The MAX-DOAS technique can derive the vertical distribution and column amount for aerosols and gases by utilizing the inversion analysis of scattered sunlight spectra measured at multiple viewing elevation angles. When MAX-DOAS observations are made, the line of sight must be clear at all elevation angles selected for the observations. In addition, there is the need for sufficient electric power, limiting the observation site. To solve these limitations, we developed the new instrument, called Eco-MAXDOAS, using the photovoltaics as a power source. For this development, we removed a temperature controller to reduce the power consumption. Instead, a shutter was introduced just before the entrance slit of the spectrometer. With this modification, it was made possible to take dark count measurements more often than for the normal MAX-DOAS instrument by closing the shutter between observations at different elevation angles. We tested the Eco-MAXDOAS and found that the spectrometer temperature changed by less than  $\pm 0.3$  degrees for 3 min. interval of changing elevation angles. Using dark count data obtained before and after a scattered sunlight observation was made, the SNR was estimated to be about 10000. This supports that analysis for a differential absorption as small as  $10^{-4}$  (0.01%) is possible. In addition, we conducted continuous observations using 30-W and 60-W solar panels. When the 30-W solar panel was used, the Eco-MAXDOAS terminated in few days. On the other hand, using the 60-W solar panel prolonged the operation time period and the Eco-MAXDOAS worked continuously for over full test observation period of two weeks under usual weather conditions in winter. In this presentation, we also assess the performance for the Eco-MAXDOAS observation by comparing aerosol and NO<sub>2</sub> data retrieved from Eco-MAXDOAS and MAX-DOAS observations.

Keywords: MAX-DOAS, solar power, aerosol, nitrogen dioxide

## Measurement of stable isotope ratios of atmospheric carbon dioxide by wavelength modulation absorption spectroscopy with

KINDAICHI, Yusuke<sup>1\*</sup> ; TONOKURA, Kenichi<sup>1</sup>

<sup>1</sup>Graduate School of Frontier Science, Tokyo University

Since the industrial revolution, the concentration of carbon dioxide, a greenhouse gas is increasing every year, it has become a cause of global warming. Carbon dioxide is released from various emission sources and is absorbed to different sinks. Carbon dioxide is circulated among the atmosphere, hydrosphere, and geosphere. For suppression global warming, there is a need to accurately grasp the emissions and removals of carbon dioxide between these reservoirs. Measurement of concentration and stable isotope ratio of carbon dioxide provide us useful information in order to elucidate the carbon cycle. Therefore, we focus on the approach to use the stable isotope as an index. Carbon dioxide has stable isotopes,  $^{12}\text{CO}_2$ ,  $^{13}\text{CO}_2$ , and  $^{12}\text{C}^{18}\text{O}^{16}\text{O}$ , it is known that these isotope ratios are different for each emission source.

As one of conventional measurement techniques of isotope ratios which has been used, there is isotope ratio mass spectrometry (IRMS) technique. Although this technique has a very high measurement precision (0.01-0.1 ‰), it cannot be measured outside the laboratory because the device is a large. Therefore, a laser absorption spectroscopy in recent years has been attracting attention. This technique is excellent in portability since the device can be made compact. Also, because suitable selection of absorption lines prevents interference from other species, the sample can be introduced directly to the device. Therefore, the device can be carried to the location where we want to measure the stable isotope ratio of carbon dioxide, it is possible to perform real-time measurements at high time resolution.

In this study, we constructed a high-precision measuring device of atmospheric carbon dioxide stable isotope ratios, using wavelength modulation absorption spectroscopy with a newly developed 2.8  $\mu\text{m}$  DFB laser and a Heriot type multi-pass reflection cell. In the measurement, absorption lines are selected in terms of being continuous of  $^{12}\text{CO}_2$ ,  $^{13}\text{CO}_2$  and  $^{12}\text{C}^{18}\text{O}^{16}\text{O}$  and small interference from water around 2.8  $\mu\text{m}$ . Wavelength modulation absorption spectroscopy allows improved sensitivity and zero background measurement by modulating wavelengths at a high frequency and performing heterodyne detection.

Keywords: carbon dioxide, stable isotope, near-infrared absorption spectroscopy

## Seasonal variation of Pb stable isotope ratio in PM observed in Yakushima Is.

NAGAFUCHI, Osamu<sup>1\*</sup> ; YOKOTA, Kuriko<sup>2</sup> ; NAKAZAWA, Koyomi<sup>1</sup> ; TETSUKA, Kenshi<sup>3</sup> ; TETSUKA, Tatsuko<sup>3</sup>

<sup>1</sup>University of Shiga prefecture, <sup>2</sup>Toyohashi University of Technology, <sup>3</sup>Society of Yakushima

A total of 36 sets of PM10 and PM2.5 aerosol particles collected from Yakushima Island during a period from January to June 2013 were determined for atmospheric Pb concentrations. Among these samples, 36 sets of samples representing two seasons, winter and spring, were selected for measuring Pb isotopic compositions to determine the relative contributions of various pollution sources. Results reveal an evident seasonality of high spring and comparatively low winter Pb concentrations, resembling those observed in Beijing, China as well as many East Asian countries. Together with synoptic atmospheric conditions analysis, the seasonal pattern is attributable to the impact of long-range transport of Pb-rich anthropogenic aerosols from the Chinese pollution outflows in the northeast monsoon. Results of  $^{206}\text{Pb}/^{207}\text{Pb}$  and  $^{208}\text{Pb}/^{207}\text{Pb}$  isotope ratios show a minimum at February, thereafter increasing progressively to March and reaching a maximum at April. From January to June, Pb isotope ratios are quite comparable with those measured in China, especially Dalian and Tianjin. Again this demonstrates Yakushima Island has already been affected by continental pollution of long-range transport during the northeast monsoon season beginning in winter and ending in late spring.

## Comprehensive analyses of air pollutants at Suzu, Noto peninsula, Japan

SADANAGA, Yasuhiro<sup>1\*</sup>; NAKAO, Yuki<sup>1</sup>; ISHIYAMA, Ayana<sup>1</sup>; TAKAJI, Ryo<sup>1</sup>; MATSUKI, Atsushi<sup>2</sup>; IWAMOTO, Yoko<sup>3</sup>; WATANABE, Koichi<sup>4</sup>; SATO, Keiichi<sup>5</sup>; OSADA, Kazuo<sup>6</sup>; BANDOW, Hiroshi<sup>1</sup>

<sup>1</sup>Osaka Prefecture University, <sup>2</sup>Kanazawa University, <sup>3</sup>Tokyo University of Science, <sup>4</sup>Toyama Prefectural University, <sup>5</sup>Asia Center for Air Pollution Research, <sup>6</sup>Nagoya University

Recent remarkable economic progress in East Asia has increased emissions of air pollutants such as nitrogen oxides, sulfur dioxide, ammonia and volatile organic compounds. Such pollutants are transported over a long distance with photochemical reactions and then arrive at Japan as aged species such as gas phase nitric acid ( $\text{HNO}_3$ ), particulate nitrate ( $\text{NO}_3^-$ ), sulfate ( $\text{SO}_4$ ), peroxy nitrates (PNs), organic nitrates (ONs), ammonium ( $\text{NH}_4^+$ ), organic aerosol (Org) and so on. Many researches on the transboundary pollution in Japan focus on the areas of western Japan near the Asian continent. On the other hand, it is important to investigate the transboundary air pollution in the central Japan area because there are many large cities. In addition, the central Japan is moderately far from the Asian continent, so that more aged air mass from the Asian continent would come at the central Japan. In this research, continuous observations of such air pollutants at Suzu, Noto peninsula, Japan. Suzu is representative remote area and located at the central Japan.

Observations are performed at NOTOGRO (NOTO Ground-based Research Observatory) supersite (37.45°N, 137.36°E) in Suzu. Total odd nitrogen species ( $\text{NO}_y$ ) and total nitrate ( $\text{T.NO}_3 = \text{HNO}_3 + \text{NO}_3^-$ ) were measured by a scrubber difference / NO-O<sub>3</sub> chemiluminescence method. PNs and ONs were measured by a thermal dissociation / cavity attenuated phase shift spectroscopy method. CO, O<sub>3</sub> and SO<sub>2</sub> were observed by non-dispersive IR, UV absorption, and pulsed UV fluorescence methods, respectively. Org,  $\text{NH}_4^+$ , SO<sub>4</sub> and fine  $\text{NO}_3^-$  were measured by an aerosol mass spectrometer. SO<sub>4</sub> was also measured by a thermal reduction / pulsed UV fluorescence method.

Results of SO<sub>4</sub> and T.NO<sub>3</sub> were reported in this abstract. The air mass origins were classified into five groups; China and Korea (CK) North China (NC), Japan (JP), Russia (RU), and Sea (S), by backward trajectory analyses. Concentrations of air pollutants from CK air mass origin were generally high. In many cases, SO<sub>4</sub> concentrations from JP were lower than those from CK, while T.NO<sub>3</sub> concentrations from JP were similar to those from CK. In addition, SO<sub>4</sub> concentrations from CK were very high, but T.NO<sub>3</sub> concentrations from CK were not, in August 2013 and June 2014. Many of SO<sub>4</sub> in remote area is present as fine particles while  $\text{NO}_3^-$  exists as coarse particles mainly. The deposition velocity of coarse particles (ca. 0.03-1.24 cm s<sup>-1</sup>) is larger than that of fine aerosols (ca. 0.05-0.6 cm s<sup>-1</sup>). In addition, the deposition velocity of HNO<sub>3</sub> (ca. 1-8 cm s<sup>-1</sup>) is larger than that of  $\text{NO}_3^-$ . The lifetime of SO<sub>4</sub> is longer than that of T.NO<sub>3</sub>, so that SO<sub>4</sub> contributes strongly to the transboundary air pollution at Suzu, in comparison with T.NO<sub>3</sub>. In this presentation, more detailed results and discussion, including other air pollutants will be described.

Keywords: Long-range transport, Air pollutants, East Asia

## Long-term observation of CCN characteristics at Suzu, Noto peninsula, Japan

MATSUKI, Atsushi<sup>1\*</sup> ; IWAMOTO, Yoko<sup>2</sup> ; KINOUCI, Kento<sup>1</sup>

<sup>1</sup>Kanazawa University, <sup>2</sup>Tokyo University of Science

Atmospheric aerosols can play a significant role in regulating radiative properties and lifetimes of clouds by acting as cloud condensation nuclei (CCN). The atmospheric concentrations of CCN are perturbed by major anthropogenic emission sources. This is particularly true in East Asia and its downwind regions which can be considered by far as one of the global hotspots of anthropogenic aerosols. Despite the regional relevance, there are still few reports on the variations of CCN properties in relation to the distinct monsoon and seasonal climate in the region.

In this study, we performed long-term monitoring of CCN activity at the remote coastal site along the Sea of Japan, namely at the tip of Noto peninsula. Such a remote geographical setting is considered ideal for characterizing CCN over extended periods with particular emphasis on the effects of typical seasonal atmospheric transport patterns and occasional outflow of atmospheric pollutants.

The measurement was conducted at the NOTOGRO (acronym for NOTO Ground-based Research Observatory) station in Suzu city (37.45 °N, 137.36 °E) at the tip of a peninsula. The PM10 inlet (14.7 m a.g.l.) provided sample air into the building for the aerosol in-situ measurements. The ambient aerosol was dried by silica-gel before entering into a differential mobility analyzer (DMA, Model 3081, TSI) for size selection. The mono-dispersed aerosol was then guided to a condensation particle counter (CPC, Model 3785, TSI) and a continuous flow thermal gradient CCN counter (CCNC, CCN-100, DMT). The CCNC was operated at four different supersaturation conditions ( $SS=0.1\%$ ,  $0.2\%$ ,  $0.5\%$ ,  $0.8\%$ ). We employed SMCA (Scanning mobility CCN analysis) method for obtaining the activation diameter  $d_{act}$  for each  $SS$  (Moore et al., Aerosol Sci. Tech., 2010) from which the hygroscopicity parameter  $\kappa$  can be derived (Peters and Kreidenweis, Atmos. Chem. Phys., 2007). The bulk chemical composition of non-refractory submicrometer-sized aerosols was also measured simultaneously by an aerosol chemical speciation monitor (ACSM, Aerodyne Inc.).

The spring and autumn months were characterized by large variation in mass and composition of CCN relevant particles. This was caused by the subsequent arrival of extra-tropical cyclone and anti-cyclone often accompanying transport of polluted continental air-mass. However, unexpectedly high concentrations of fine particles persisted even in summer period, characterized by relatively large contribution of organics. There was a rather good correlation between the abundance of organics (relative to sulfate) in the aerosol bulk chemical composition and the hygroscopicity  $\kappa$ , such that  $\kappa$  values were particularly low during the summer period.

There was a further evidence that the temporal variation in  $\kappa$  value was not in phase with org/inorg mass ratios alone, but also weakly correlated with the organic composition. Analysis of mass spectra from ACSM revealed that the oxidative state of organics also influenced the  $\kappa_{org}$ . These findings highlight the importance of the temporal variations in particle chemistry as well as their aging states for conducting CCN closure in the region.

Keywords: aerosol, CCN, Organics, Long-range transport



## Enhancement of dimethylsulfide production by anoxic stress in natural seawater

OMORI, Yuko<sup>1\*</sup>; TANIMOTO, Hiroshi<sup>1</sup>; INOMATA, Satoshi<sup>1</sup>; WADA, Shigeki<sup>2</sup>; THUME, Kathleen<sup>3</sup>; GEORG, Pohnert<sup>3</sup>

<sup>1</sup>National Institute for Environmental Studies, <sup>2</sup>University of Tsukuba, <sup>3</sup>Friedrich Schiller University Jena

Dimethylsulfide (DMS) is the dominant reduced sulfur species in the ocean and an important source of aerosols particles and clouds in the marine atmosphere. Marine DMS plays a key role in the climate system of the Earth. A better knowledge of the distribution of marine DMS and its controlling factors is required. Previous field studies have reported the formation of DMS peak upper anoxic layer though the governing processes have not been clearly understood yet. Here we show the first direct evidence for the enhancement of DMS production caused by anoxic stress.

Isotope tracer experiments were made using the oxic and anoxic coastal seawater to quantitatively evaluate DMS production rates in three processes; cleavage of dimethylsulfoniopropionate (DMSP), dimethylsulfoxide reduction and phytoplankton release.

Under the anoxic condition, DMS production was considerably enhanced and DMS consumption was inhibited, resulting in an 8-fold higher rate of gross DMS production than that under the oxic condition. While almost all DMS was derived from DMSP cleavage (99%) under the oxic condition, the DMS production under the anoxic condition was mainly due to direct release of DMS from phytoplankton (63%). These results demonstrate that phytoplankton suffered from anoxic stress emits DMS into the seawater, resulting in a rise in DMS levels. Anoxic stress is indicated to be one of important environmental factors in the dynamics of marine DMS, suggesting the possible global importance due to a ubiquity of anoxic conditions in the coastal oceans.

Keywords: dimethylsulfide, dimethylsulfoniopropionate, dissolved oxygen

## Atmospheric hydrogen measurements in the western North Pacific

TSUBOI, Kazuhiro<sup>1\*</sup>; MATSUEDA, Hidekazu<sup>1</sup>; SAWA, Yousuke<sup>1</sup>; NIWA, Yosuke<sup>1</sup>; TAKATSUJI, Shinya<sup>2</sup>; FUJIWARA, Hiroaki<sup>2</sup>; DEHARA, Kohshiro<sup>2</sup>; OKUDA, Tomoki<sup>2</sup>; MORI, Yoki<sup>2</sup>

<sup>1</sup>Meteorological Research Institute, <sup>2</sup>Japan Meteorological Agency

Molecular hydrogen (H<sub>2</sub>) plays a significant role in global atmospheric chemistry due to its role in CH<sub>4</sub>-CO-OH cycling and water vapor source in the stratosphere. The balance of H<sub>2</sub> could change with the implementation of a new H<sub>2</sub> energy carrier. Therefore, it is important to establish its global budget and atmospheric trend (WMO/GAW Report No.197, 2011).

We started atmospheric H<sub>2</sub> measurement at Minamitorishima (MNM) from Nov. 2011. The measurement system using a GC-RGD (gas chromatographs equipped with a reduction gas detector) was installed for simultaneous analyses of H<sub>2</sub> and carbon monoxide at 3 stations of MNM, Yonagunijima (YON), and Ryori (RYO) operated by Japan Meteorological Agency (JMA). In this study, high-precision H<sub>2</sub> standard gases are prepared to determine the atmospheric concentrations from the output signal of the GC/RGD.

The H<sub>2</sub> concentrations at MNM varied seasonally from 490 ppb to 560 ppb with a yearly mean of about 520 ppb. The H<sub>2</sub> variations often show distinct episodic events with enhanced concentrations on a synoptic scale in winter. This result indicates that H<sub>2</sub> increases are caused by the long-range transport of Asian polluted air masses to the station, suggesting that H<sub>2</sub> is a good tracer for identifying continental air masses in winter season. On the other hand, the H<sub>2</sub> concentrations are higher and stable in summer season. This result indicates that the maritime air masses are dominated, and the influence of soil absorption was small.

Keywords: hydrogen

## Observation of optical and chemical properties of aerosols at a forest site in Kii Peninsula during summer of 2014

KUBODERA, Ryo<sup>1\*</sup>; NAKAYAMA, Tomoki<sup>2</sup>; KAGAMI, Sara<sup>3</sup>; DENG, Yange<sup>3</sup>; OGAWA, Shuhei<sup>3</sup>; MOCHIDA, Michihiro<sup>3</sup>; ADACHI, Kouji<sup>4</sup>; AOKI, Kazuma<sup>5</sup>; MATSUMI, Yutaka<sup>2</sup>

<sup>1</sup>Graduate School of Science, Nagoya University, <sup>2</sup>Solar-Terrestrial Environment Laboratory, Nagoya University, <sup>3</sup>Graduate School of Environmental Studies, Nagoya University, <sup>4</sup>Meteorological Research Institute, Japan Meteorological Agency, <sup>5</sup>Faculty of Science, University of Toyama

Aerosols scatter and absorb solar radiation and influence to the radiation balance in the atmosphere. Forests are a significant source of both primary biological aerosol particles (PBAPs) and biogenic secondary organic aerosols (BSOAs). In addition, polluted air masses including sulfate and black carbon (BC) particles may also be long range transported to forest areas in Japan. If the BC particles were coated with inorganic and/or organic materials during the long-range transport, the light absorption of BC could be enhanced due to the lensing effect. However, relations of aerosol optical properties including lensing effect with chemical properties of aerosols in Asian forest area have not been well understood. In this work, optical and chemical properties of aerosols were simultaneously measured in a forest site in Japan.

The observations were conducted from 17 July to 3 September 2014 at the Wakayama Forest Research Station, Kyoto University, Japan (34.06N, 135.52E, around 535 m above sea level), which is located in the central part of Kii Peninsula. Ambient particles were sampled from an inlet placed at 6.4 m above ground level. Absorption and scattering coefficients of PM<sub>1</sub> particles were measured using two photoacoustic spectrometers (PASS-3 at  $\lambda = 405, 532, 781$  nm and PAX at  $\lambda = 375$  nm, DMT) after passing aerosols through a heater controlled at 300 °C or a bypass line by switching ball valves every 10 min. By comparing absorption coefficients at 781 nm with and without heating, increase in BC light absorption due to coating can be estimated. Mass concentrations of non-refractory materials were measured using an aerosol mass spectrometer (AMS, Aerodyne Research). Mass concentrations of elemental carbon (EC) and organic carbon (OC) were also measured by thermo-optical technique using a semi-continuous EC/OC analyzer (Sunset Lab.). Size distributions of particles were measured using a scanning mobility particle sizer (SMPS, TSI) and optical particle counters (OPCs, RION and TSI). Aerosol particles were also collected using an impactor for morphological analysis using a transmission electron microscope (TEM). Optical thickness (AOT) and extinction Angstrom exponent of aerosols were also measured using a Skyradiometer (Prede). In the presentation, relation between the obtained optical properties with chemical and physical properties of aerosols will be discussed.

Keywords: Aerosol optical property, Ambient measurement, Forest site, Biogenic SOA, Lensing effect, Photoacoustic spectroscopy

## Chemistry with KROME: Dynamical photochemical solver coupled to chemical disequilibrium and sulfur isotopes

DANIELACHE, Sebastian<sup>1\*</sup>

<sup>1</sup>Sophia University Faculty of Science and Technology Department of Materials and Life Science

The study of chemical networks of Earth's geological past such as the Archean and Exoplanetary atmospheres requires the resolution of a large number of chemical reactions. This necessity is based on the lack of observational parameters abundant in today's planet Earth or neighbor planets in the solar system. The aim of this work is to construct a planetary atmosphere chemical network solver that relies on a minimal number of observational parameters.

We present here the latest development in our effort to develop such model. Our previous report presented the efficiency of the chemical solver for a large number of chemical species and reaction networks. In this report we present a photochemical dynamic core capable of solving ultraviolet opacities and photo-dissociation reaction rates at each step of the calculation. Additionally the model has been equipped with a set of equations to calculate disequilibrium effects on the chemical network. The stability and robustness of the code has been tested for a large network with more than 500 reactions interlinking more than 40 chemical species. The results obtained so far have been contrasted with the most common chemical codes available in the literature for benchmark.

Keywords: Archean Atmosphere, Sulfur Isotopes

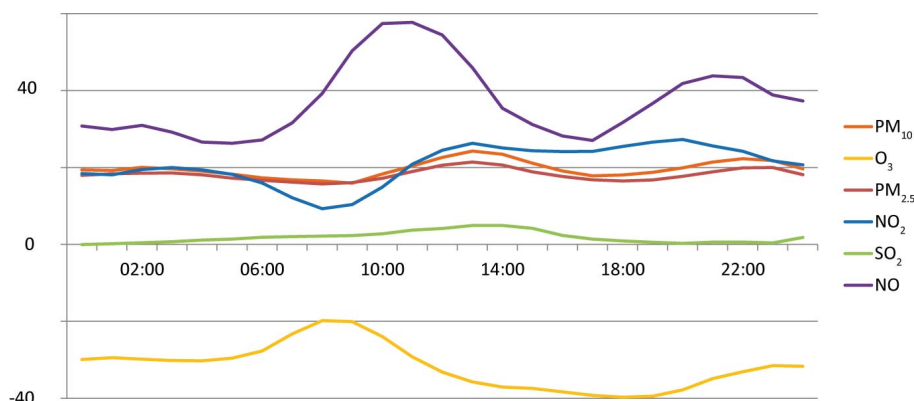
## Urban fog and atmospheric pollution: contrasted effects on pollutants in Lyon (France)

RENARD, Florent<sup>1\*</sup> ; FUJIKI, Kenji<sup>1</sup>

<sup>1</sup>University Jean Moulin Lyon 3, UMR 5600

Lyon (500 000 inhabitants), located in the southeastern France, is an industrial city, with a polluted atmosphere and many days of fog. This unfavorable atmospheric situation poses many health problems to people and harms the attractiveness of the city and the development of trade. Greater Lyon has the highest levels of fine particulates and nitrogen dioxide in the Rhone-Alpes region and is prosecuted by the European Union for non-compliance with the Directive of 21 May 2008 concerning the quality of ambient air and cleaner air for Europe. This area is disadvantaged by its geographical situation, with the presence of two major rivers (Rhone and Saone) and many reliefs, influencing the conditions of dispersion of pollutants in the atmosphere and makes the Lyon an atmospherically sensitive city, despite prevailing winds North-South or South-North oriented which tend to favor the dispersion of pollutants. In addition, Lyon concentrates pollution from traffic, industrial, and tertiary sectors. In winter, temperature inversions (temperature higher in altitude than on the ground) promote stagnation of pollutants at low altitude. This phenomenon is amplified considerably during episodes of urban mist. As a first step, the evolution of the number of foggy days is studied, and explanatory factors are proposed. The months of October to January are the most affected, with an average of 7 days of fog in December and January, over the period 1949-2013. It is thus noticed a steady decline in the number of foggy days since 1921 until early 2000s, from more than 90 days to only fifteen, followed by stagnation and a slight increase in recent years. This trend is compared to the annual minimum temperatures of Lyon, following an opposite trend, with an increase until the late 2000s, from 6 degrees C to 9 degrees C, followed by a stagnation and a slight decrease. A strong relationship is obtained between these two parameters, but the average wind speed may also explain the decrease, limiting conditions for fog formation, with a more important mixing of the air. Again, it can be noticed an increase in the average wind speed and in the proportion of winds faster than 1 m / s until the early 2000s, and then a decrease. Finally, better controls of industrial air emissions also explain the decrease in the number of days with fog over the long term. In a second step, the concentrations of air pollutants (PM10, PM2.5, O3, NO2, NO and SO2) are studied with and without fog. A station in the center of the city records these pollutants since 2007 continuously, every hour. In 2013, during foggy days and comparatively to clear days, it is found a strong increase in PM 10 and PM 2.5, respectively from 22.3  $\mu\text{g.m}^{-3}$  and 16.8  $\mu\text{g.m}^{-3}$  to 39.7  $\mu\text{g.m}^{-3}$  and 33  $\mu\text{g.m}^{-3}$ , above recommended thresholds. Concentrations of nitric oxide (NO) and nitrogen dioxide (NO2) are respectively 9.0  $\mu\text{g.m}^{-3}$  and 27.7  $\mu\text{g.m}^{-3}$  during clear days, passing to 52.8  $\mu\text{g.m}^{-3}$  and 50.5  $\mu\text{g.m}^{-3}$  during foggy days, exceeding the recommended values here too. And inversely, as a result of sunlight blocking by water droplets in suspension, there is a decrease in O3, from 42.4  $\mu\text{g.m}^{-3}$  to 13.9  $\mu\text{g.m}^{-3}$ , while the SO2 remains stable and very low, at 1.2  $\mu\text{g.m}^{-3}$  (fig. 1). These observations made in 2013 are the same since 2007. Finally, the evolution of the concentration of PM 10 is studied during persisting foggy days, hours after hours. There is a steady and dramatic increase in the concentration with consecutive days of fog, going to an increase of 40  $\mu\text{g.m}^{-3}$  on the fourth day. In conclusion, air pollution in urban areas under clear skies is already a major concern, but the action of the latter on health is particularly worrying during episodes of urban smog.

Keywords: fog, atmospheric pollution, particulate matter, Lyon, France



Average hourly evolution of pollutant concentrations ( $\mu\text{g.m}^{-3}$ ) during foggy days, compared to standard days (Lyon city center, France ; 2007-2013)

## Impacts of weather regimes on PM10 pollution peaks in Rhone-Alpes (France)

RENARD, Florent<sup>1\*</sup> ; FUJIKI, Kenji<sup>1</sup>

<sup>1</sup>University Jean Moulin Lyon 3, UMR 5600

Pollution in particulate matter is a more and more significant problem, especially in urban areas, and widely publicized when regulatory thresholds are exceeded. Health consequences have to be carefully considered, for both short-term and long-term effects. First, this paper describes the spatial and temporal distribution of PM10 concentrations (particulate matter with a diameter inferior to 10  $\mu\text{m}$ ) in urban environments in the Rhone-Alpes administrative area, located in South-east France. Pollution monitoring stations are grouped together by ascending hierarchical classification. The goal is to identify similar patterns on a regional scale. Then, this PM10 distribution is analyzed according to synoptic-scale weather regimes. As the classic analysis between anticyclonic and cyclonic types appears insufficient, particulate matter concentrations are related to weather regimes according to Hess-Brezowsky classification system, which is widely used in Western Europe for numerous climate studies. The latter has been chosen after a review of the existing European classifications, and this analysis is one of the first to be made in France. Results show that strong annual disparities are observed amongst the different urban monitoring stations in Rhone-Alpes on both spatial and temporal scales. More precisely, stations in deep alpine valleys and in the regional capital city Lyon are the most polluted ones. Concerning monthly means, the most polluted months are obviously those in winter, due to the emitting sources considered. Steepest gaps are nonetheless better observed on an hourly basis, with two peaks at the end of the morning and at early evening. When analyzed according to the weather regimes, high pressure area over Central Europe weather regimes are prevailing during information and alert thresholds exceedances. More specifically, six regime types (Groswwetterlagen) are strongly associated with pollution peaks. Two are cyclonic (WZ and NWZ) and their persistence during several consecutive days leads to a decrease in pollution. They are only associated with pollution peaks because they have represented a large part of global circulation during the last few years. By contrast, the most worrying regime types in regard with pollution peaks are anticyclonic : SWA, WA, HM, and BM. Those last two types, when persisting over several days, lead to a steep increase in pollutant concentrations.

Keywords: particulate matter, pollution peaks, weather regimes, Hess-Brezowsky, Lyon, France

## Height-resolved measurements of the aerosol size distributions in a temperate forest by tower observation system

TAKAHASHI, Kenshi<sup>1\*</sup> ; YABUKI, Masanori<sup>1</sup> ; MATSUDA, Kazuhide<sup>2</sup> ; TSUDA, Toshitaka<sup>1</sup>

<sup>1</sup>RISH, Kyoto University, <sup>2</sup>Faculty of Agriculture Field Science Center, Tokyo University of Agriculture and Technology

Dry and wet depositions are quite important for aerosol particles to be removed from the atmosphere. Also deposition of ammonium, sulfate, and nitrate contained in aerosol particles may contribute to potential acidification and eutrophication of the ecosystems. Both deposition processes are size specific, in particular, dry deposition of aerosol particles depends principally on particle size, atmospheric turbulence and stability and the collecting properties of the surface.

We conducted observational studies measuring the number size distributions of ambient submicron and ultrafine aerosol particles in a deciduous forest, during the summers of 2013 and 2014. The deciduous forest is located in suburban Tokyo, as a part of the experimental forest at the Tokyo University of Agriculture and Technology (Field Museum Tamakyuryo (FM Tama)). The observation site has a 30-m tall tower where we installed aerosol measurement instruments of the Scanning Mobility Particle Sizer and the Optical Particle Counter to explore the vertical profiles of the aerosol size distributions within and above the forest canopy. We report that the size distribution for submicron particles varied significantly with both temporally and vertically, depending on the wind field as well as the relative humidity related to the hygroscopic properties of aerosol particles.

Keywords: atmospheric aerosol, size distributions, tower observation

## Direct measurements of photochemical ozone production rate at a forest area in Japan during summer of 2014

KAWASAKI, Shio<sup>1\*</sup>; SADANAGA, Yasuhiro<sup>1</sup>; TSURUMARU, Hiroshi<sup>2</sup>; IDA, Akira<sup>2</sup>; KISHIMOTO, Iori<sup>2</sup>; KAJII, Yoshizumi<sup>2</sup>; NAKAYAMA, Tomoki<sup>3</sup>; BANDOW, Hiroshi<sup>1</sup>

<sup>1</sup>Osaka Prefecture University, <sup>2</sup>Kyoto University, <sup>3</sup>Nagoya University

We developed a direct measurement system of photochemical ozone production rate in order to evaluate ozone concentration variations quantitatively. In fact, this system measures oxidant ( $Ox = O_3 + NO_2$ ) production rate. The use of Ox can ignore the concentration variations of  $O_3$  due to titration of  $O_3$  by NO. The field campaign was performed at Wakayama, a remote site, in Japan during summer of 2014. Measurement parameters were photochemical net Ox production rate ( $P-L(Ox)$ ),  $[O_3]$ ,  $[NO]$ ,  $[NO_2]$ ,  $[RO_2]$ ,  $[VOCs]$ , OH reactivity, photolysis frequencies of various trace species and so on.

The  $P-L(Ox)$  measurement system has "reaction" and "reference" chambers. The reaction and reference chambers (17.1-cm inner diameter and 50-cm length) are made of quartz and Pyrex, respectively. Inner walls of both the chambers are coated with clear Teflon films to avoid wall loss of  $O_3$ . An outer wall of the reference chamber is coated with a UV-cut film (50% cutoff wave length of 405 nm). Both the chambers were put in an outdoor location to be exposed directly to sunlight. Ambient air is introduced into both the chambers. In the reaction chamber, photochemical reactions proceed to generate Ox. On the other hand, Ox is not generated in the reference chamber. The difference of Ox concentrations ( $\Delta Ox$ ) in air from the two chambers is the Ox produced by photochemical reactions in the reaction chamber. The  $P-L(Ox)$  is obtained by dividing  $\Delta Ox$  by a mean residence time of air in the reaction chamber. Ox concentrations were obtained as follows.  $O_3$  in Ox is converted into  $NO_2$  by the reaction of  $O_3$  with large excess of NO, and then the  $NO_2$  concentration is measured by a laser-induced fluorescence technique.

The field campaign was conducted at Field Science Education and Research Center, Kyoto University, Wakayama Forest Research Station, in Wakayama Prefecture, Japan. Observation site is in forest area and anthropogenic sources of air pollutants are very low. Observations were conducted from 28 July to 8 August. Most periods of the campaign,  $O_3$  concentrations were approximately 10 ppbv in the daytime.  $NO_x (= NO + NO_2)$  concentrations were less than about 1 ppbv throughout the campaign. BVOCs (Biogenic Volatile Organic Compounds) concentrations were high. Results of  $P-L(Ox)$  and Ox concentration on 6 August were reported in this abstract. A diurnal variations were observed for  $P-L(Ox)$  and Ox concentration, and the maximum rate and concentration were observed around noon. Ox concentration increased in the early morning, while  $P-L(Ox)$  was still 0 ppbv  $h^{-1}$  and then increased after a few hours. This result shows that  $O_3$  concentration is increased by non-photochemical factors in the early morning. Vertical mixing of air is weak at night and  $O_3$  concentration near the surface of the ground decreases by deposition, reactions with olefin and so on. Surface of the ground is gradually warmed by sunlight in the morning and vertical mixing of air is activated.  $O_3$  concentration would increase because of  $O_3$  influx from above.  $P-L(Ox)$  achieved a peak value around noon and photochemical  $O_3$  production was active in the daytime. Ox concentration did not increase around noon, however. This suggests that  $O_3$  increase by photochemical production competes against  $O_3$  decrease by non-photochemical factors such as deposition, advection, and reactions of  $O_3$  with olefin.

Keywords: photochemical ozone production rate, oxidant, forest area



## A global trend map of seasonal total column ozone using a MIROC3.2 nudged Chemistry-Climate Model

OBAMA, Risa<sup>1\*</sup> ; AKIYOSHI, Hideharu<sup>1</sup> ; KADOWAKI, Masanao<sup>1</sup> ; YAMASHITA, Yousuke<sup>1</sup>

<sup>1</sup>National Institute for Environmental Studies, <sup>2</sup>Atmospheric and Ocean Research Institute, The University of Tokyo, <sup>3</sup>Japan Atomic Energy Agency

We created a global trend map of seasonal total column ozone using the results of two CCM experiments to examine the influence of CFC on global total column ozone. The model used is the MIROC3.2 Chemistry-Climate Model nudged toward ERA-Interim reanalysis data. We performed two experiments. One experiment (REF-C1SD) uses observed ozone depleting substance (ODS) and greenhouse gas (GHG) concentrations that changes with time. In the other experiment (SEN-fODS1979), ODS concentration is fixed to the 1979 value. The REF-C1SD experiment shows a large decreasing seasonal total column trend globally during the CFC decreasing period (1979-1996). The trends have clear longitudinal structures at winter mid-latitudes and spring polar region.

Comparing the result of the REF-C1SD experiment with that of the SEN-fODS1979 experiment, the contributions of ODS and other processes except for ODS (for example, trends in ozone transport) are analyzed globally. We also show the trend map for the ODS decreasing period (1997-2011).

Keywords: Total Column Ozone, Trend, Chemistry-Climate Model, Global Map, ERA-Interim

## Trend analysis of satellite observed tropospheric NO<sub>2</sub> vertical column density over East Asia

MUTO, Takuya<sup>1\*</sup> ; IRIE, Hitoshi<sup>2</sup> ; ITAHASHI, Syuichi<sup>3</sup>

<sup>1</sup>Graduate School of Advanced Integration Science, Chiba University, <sup>2</sup>Center for Environmental Remote Sensing, Chiba University, <sup>3</sup>Central Research Institute of Electric Power Industry

Nitrogen dioxide plays a central role in the atmospheric environment as a toxic substance for respiratory system and precursors of ozone and aerosols. Furthermore, OH concentration is dependent on nitrogen dioxide concentration in the atmosphere. Although Hilboll et al.(2013) showed an increase in NO<sub>2</sub> concentration over Central Eastern China(CEC) until 2011 and a gradual decrease in NO<sub>2</sub> concentration over Japan until 2011, the latest trend until 2014 has not been reported yet. The time period is of interest, because it corresponds to the 12th 5-year-plan regulating NO<sub>x</sub> emissions in China and the period with the power substitution of thermal power generation for the nuclear power generation in Japan. In this study, we used two satellite datasets from OMI and GOME-2 that have been operationally observing tropospheric NO<sub>2</sub> VCD in recent years until 2014. Tropospheric NO<sub>2</sub> VCD trends in China and Japan were estimated based on the regression analysis for annual mean values. Although an increase in NO<sub>2</sub> VCD occurred at a rate of 7% per year from 2005 to 2011 over Central Eastern China, we found a decrease at a rate of 11% per year from 2011 to 2014. Over Japan, the NO<sub>2</sub> VCD increased at a rate of 4% per year from 2005 to 2011 and decreased from 2011 to 2014 at a rate of 4% per year. In this presentation, we also conduct detail trend analysis on a grid basis to discuss the potential causes for these variations in NO<sub>2</sub> VCD over China and Japan.

Keywords: Nitrogen dioxide, OMI, GOME-2, trend analysis

## CH<sub>4</sub>, H<sub>2</sub>O, N<sub>2</sub>O, and temperature from the mid-troposphere to the stratosphere in the northern mid- and high-latitudes

SUGITA, Takafumi<sup>1\*</sup> ; SAITOH, Naoko<sup>2</sup> ; HAYASHIDA, Sachiko<sup>3</sup> ; MACHIDA, Toshinobu<sup>1</sup>

<sup>1</sup>NIES, <sup>2</sup>Chiba Univ., <sup>3</sup>Nara Women's Univ.

Profiles of CH<sub>4</sub> have been retrieved from satellite-borne nadir sensors since 1996 by measuring thermal infrared (TIR) emissions from the Earth's atmosphere. GOSAT/TANSO-FTS has been operated since 2009. Profiles of CO<sub>2</sub> and CH<sub>4</sub> are retrieved from the TIR band of the TANSO-FTS. In this study, we assess data quality for CH<sub>4</sub>, H<sub>2</sub>O, N<sub>2</sub>O, and temperature between the mid-troposphere and the stratosphere, contributing the improvement of our knowledge on CH<sub>4</sub> distributions, for instance, in the western Siberia. For comparisons with the TIR data, we used the solar occultation sensor, ACE-FTS, and the routine aircraft observations in the western Siberia. We found that (1) TIR CH<sub>4</sub> mixing ratios are systematically larger than ACE-FTS CH<sub>4</sub> in the 400-200 hPa levels between January and April in 2010/2011, especially in January, several profiles exceeded 2.0 ppmv of CH<sub>4</sub> at the 300 hPa level. (2) TIR H<sub>2</sub>O mixing ratios are larger than ACE-FTS H<sub>2</sub>O in the 300-250 hPa levels and the above throughout the period studied. (3) TIR CH<sub>4</sub> at the 7 km (430 hPa) and the 5.5 km (500 hPa) altitudes are in good agreement with those from the aircraft observations from the temporal variation view within the range of variations in TIR CH<sub>4</sub>.

Acknowledgements: We thank Kaley A. Walker, University of Toronto, Canada for providing us the Version 3.5 ACE-FTS data through <http://ace.uwaterloo.ca>. This research was supported by the Environment Research and Technology Development Fund (ERTDF) of the Ministry of the Environment, Japan (A1202). Aircraft observations in the western Siberia are conducted by NIES with the cooperation of Russian Academy of Science (RAS).

Keywords: methane, troposphere, stratosphere, GOSAT, aircraft

## Comparisons between NICAM-TM and GOSAT/TANSO-FTS TIR CO<sub>2</sub> data

SUGIMURA, Ryo<sup>1\*</sup> ; SAITOH, Naoko<sup>1</sup> ; IMASU, Ryoichi<sup>2</sup> ; KAWAKAMI, Shuji<sup>3</sup> ; SHIOMI, Kei<sup>3</sup> ; NIWA, Yosuke<sup>4</sup> ; MACHIDA, Toshinobu<sup>5</sup> ; SAWA, Yousuke<sup>4</sup> ; MATSUEDA, Hidekazu<sup>4</sup>

<sup>1</sup>Center for Environmental Remote Sensing, Chiba University, <sup>2</sup>Atmosphere and Ocean Research Institute, The University of Tokyo, <sup>3</sup>Japan Aerospace Exploration Agency, <sup>4</sup>Meteorological Research Institute, <sup>5</sup>National Institute for Environmental Studies

Greenhouse gases Observing SATellite (GOSAT), which was the first satellite for global observations of greenhouse gases, was successfully launched on 23 January 2009. Our recent analysis suggested that CO<sub>2</sub> vertical profiles retrieved from Thermal and Near Infrared Sensor for Carbon Observation (TANSO) - Fourier Transform Spectrometer (FTS) thermal infrared (TIR) band had a negative bias in the middle troposphere. In this study, we globally evaluated the magnitude of the bias through the comparisons between the TIR CO<sub>2</sub> data and Nonhydrostatic Icosahedral Atmospheric Model - based Transport Model (NICAM-TM) CO<sub>2</sub> data [Niwa et al., 2011]. Furthermore, we calculated a correction factor to modify the bias for each latitude band and applied the latitude-dependent correction factors to the TIR CO<sub>2</sub> data on 500 hPa; here, we estimated the correction factors on the basis of comparisons between CO<sub>2</sub> profiles observed over airports by Continuous CO<sub>2</sub> Measuring Equipment (CME) in Comprehensive Observation Network for Trace gases by Airliner (CONTRAIL) project [Machida et al., 2008] and the coincident TIR CO<sub>2</sub> profiles. Then, we analyzed seasonal variations of the modified TIR CO<sub>2</sub> data to check the validity of the correction factors estimated here.

Comparisons of the differences of CO<sub>2</sub> concentrations on 500 hPa and 200 hPa (500 hPa minus 200 hPa) between TIR CO<sub>2</sub> data and NICAM-TM CO<sub>2</sub> data showed that the differences of the TIR CO<sub>2</sub> data were larger than those of the NICAM-TM CO<sub>2</sub> data because of the negative bias of the mid-tropospheric TIR data. The CO<sub>2</sub> differences between the two pressure levels of the TIR data were particularly large (~8 ppmv) in low latitudes; this characteristic was not seen both in the NICAM-TM CO<sub>2</sub> data and the a priori CO<sub>2</sub> data (NIES-TM05). Next, we applied the latitude-dependent correction factors to the TIR CO<sub>2</sub> data on 500 hPa, and then compared the CO<sub>2</sub> differences on 500 hPa and 200 hPa. In low latitudes (25° S-25° N), the CO<sub>2</sub> differences between the two pressure levels of the TIR data became closer to the CO<sub>2</sub> differences of the NICAM-TM CO<sub>2</sub> data and the a priori CO<sub>2</sub> data when we applied the correction factor estimated over Bangkok. On the other hand, in northern high latitudes (northern latitudes of ~40° N), most of the CO<sub>2</sub> differences between the two pressure levels of the TIR data were positive unlike the NICAM-TM CO<sub>2</sub> and the a priori CO<sub>2</sub> data when we applied the correction factor estimated over Amsterdam. In boreal summer, surface CO<sub>2</sub> concentrations are lower than middle and upper tropospheric CO<sub>2</sub> concentrations; in that sense, the correction factor applied here was not appropriate in northern high latitudes in summer. These results suggest that the magnitude of the negative bias seen in TIR CO<sub>2</sub> data would vary depending on seasons as well as regions, and therefore, we should estimate a latitude-dependent correction factor for each season.

Furthermore, we compared time series of TIR CO<sub>2</sub> data with those of NICAM-TM CO<sub>2</sub> data and the a priori CO<sub>2</sub> data for several different regions that were categorized in terms of climatic divisions and latitude bands [Niwa et al., 2011]. Our preliminary results showed that the seasonal variations of the TIR CO<sub>2</sub> data in some regions were closer to those of the NICAM CO<sub>2</sub> data than of the a priori CO<sub>2</sub> data. For future work, we should review how to compare the three CO<sub>2</sub> data sets, and then closely analyze the differences in seasonal variations among the three data sets globally.

### Acknowledgements

We thank the staff and engineers of Japan Airlines, the JAL Foundation, and JAMCO Tokyo for supporting the CONTRAIL project.

Keywords: CO<sub>2</sub>, satellite remote sensing, GOSAT

## Validation of GOSAT/TANSO-FTS TIR CO<sub>2</sub> profiles using aircraft CO<sub>2</sub> data

KIMOTO, Shuhei<sup>1\*</sup> ; SAITOH, Naoko<sup>1</sup> ; IMASU, Ryoichi<sup>2</sup> ; KAWAKAMI, Shuji<sup>3</sup> ; SHIOMI, Kei<sup>3</sup> ;  
MACHIDA, Toshinobu<sup>4</sup> ; SAWA, Yousuke<sup>5</sup> ; MATSUEDA, Hidekazu<sup>5</sup> ; UMEZAWA, Taku<sup>4</sup>

<sup>1</sup>Center for Environmental Remote Sensing, Chiba University, <sup>2</sup>Atmosphere and Ocean Research Institute, The University of Tokyo, <sup>3</sup>Japan Aerospace Exploration Agency, <sup>4</sup>National Institute for Environmental Studies, <sup>5</sup>Meteorological Research Institute

Greenhouse gases Observing SATellite (GOSAT) was launched on 23 January 2009 to observe major greenhouse gases such as CO<sub>2</sub> and CH<sub>4</sub>. Thermal and Near-infrared Sensor for Carbon Observation Fourier Transform Spectrometer (TANSO-FTS) on board the GOSAT can observe CO<sub>2</sub> profiles in the thermal infrared (TIR) region, but the quality of the retrieved CO<sub>2</sub> profile data has not yet been fully validated. In this study, we compared GOSAT/TANSO-FTS TIR CO<sub>2</sub> profiles with aircraft CO<sub>2</sub> data to evaluate their quality. The aircraft data we used were obtained by Comprehensive Observation Network for Trace gases by Air-line (CONTRAIL) project and Civil Aircraft for the Regular investigation of the atmosphere Based on an Instrument Container (CARIBIC) project, both of which are commercial airliner projects.

First, we assumed CONTRAIL data obtained during ascending and descending flights over airports as a "CO<sub>2</sub> profile", and then compared TIR CO<sub>2</sub> profiles with the CONTRAIL CO<sub>2</sub> profiles to which the TIR averaging kernel functions were applied. We adopted a distance between the GOSAT observation and the airport within 300 km and a time difference between the two observations within 72 hour as criteria for the comparison. Here, we used the CONTRAIL profile data obtained over the ten airports: Moscow, Amsterdam, Vancouver, Narita, Delhi, Honolulu, Bangkok, Singapore, and Djakarta. We also used CONTRAIL and CARIBIC level flight data to validate the global distributions of TIR upper tropospheric CO<sub>2</sub> data. We divided the level flight aircraft data into several regions, and then compared the averaged aircraft data with the averaged TIR data in each region.

From the CO<sub>2</sub> profile comparisons at each airport, we found the TIR data had a low bias of 1-1.5%. The magnitude of the bias varied depending on seasons and latitudes; in spring and summer in low latitude, the magnitude of the bias was larger than that in autumn and winter in mid and high latitudes. From the upper tropospheric CO<sub>2</sub> comparisons, the TIR data showed better agreements to the aircraft data than the a priori data, and the distribution of the TIR upper tropospheric CO<sub>2</sub> data had a similar pattern to the distribution of the aircraft data. In the poster, we will also report the details of the comparisons using other aircraft data.

### Acknowledgements

We thank the staff and engineers of Japan Airlines, the JAL Foundation, and JAMCO Tokyo for supporting the CONTRAIL project. CARIBIC data used in this study were provided by the CARIBIC project. We also thank Dr. C. Brenninkmeijer and other members of the CARIBIC project.

Keywords: GOSAT, validation, CO<sub>2</sub>, aircraft measurement

## Climatology of spatiotemporal variations of tropospheric CO<sub>2</sub> observed by CONTRAIL-CME

UMEZAWA, Taku<sup>1\*</sup> ; MACHIDA, Toshinobu<sup>1</sup> ; SAWA, Yousuke<sup>2</sup> ; MATSUEDA, Hidekazu<sup>2</sup> ; NIWA, Yosuke<sup>2</sup>

<sup>1</sup>National Institute for Environmental Studies, <sup>2</sup>Meteorological Research Institute

CONTRAIL is the ongoing project that measures atmospheric trace gases during intercontinental flights of Japan Airlines. Atmospheric CO<sub>2</sub> concentration is analyzed using Continuous CO<sub>2</sub> Measuring Equipment (CME) onboard the aircraft. From ~20 thousands of measurement flights since 2005, extensive number of CO<sub>2</sub> data (~2 millions) along level-flight and ascent/descent tracks have been obtained, enabling us to well characterize spatiotemporal distributions of atmospheric CO<sub>2</sub> covering large part of the globe especially the Asia-Pacific regions. In this study, we define  $\Delta\text{CO}_2$  as a deviation from the long-term trend observed at a northern hemispheric baseline station Mauna Loa, Hawaii, to illustrate climatological CO<sub>2</sub> distributions including seasonal and shorter-term variations. For instance, over airports in Japan,  $\Delta\text{CO}_2$  reaches seasonal maximum at the end of April with higher values near the surface. In this season, high  $\Delta\text{CO}_2$  spreads east of the Asian continent in the upper troposphere over the northern Pacific. In contrast, seasonal minimum of  $\Delta\text{CO}_2$  occurs in September with more depletion in the upper troposphere. The summertime low  $\Delta\text{CO}_2$  in the upper troposphere appears to be more pronounced over the Asian continent than over the Pacific. Likewise, we present seasonal variations of vertical profiles of tropospheric  $\Delta\text{CO}_2$  over various airports and of spatial distributions in the upper troposphere in large-scale perspective, and discuss them from viewpoints of seasonally varying continental sources/sinks and atmospheric transport.

Keywords: CONTRAIL, CO<sub>2</sub>, troposphere, seasonal variation, vertical profile